Adsorption performance and mechanisms of mercaptans removal from gasoline oil using core-shell AC-based adsorbents: Role of intra-particles space

Pamphile Ndagijimana
Institute of Urban Environment Chinese Academy of Sciences
Xuejiao Liu
Institute of Urban Environment Chinese Academy of Sciences
Zhiwei Li
Institute of Urban Environment Chinese Academy of Sciences
Zhenjiao Xing
Institute of Urban Environment Chinese Academy of Sciences
Beibei Pan
Institute of Urban Environment Chinese Academy of Sciences
Guangwei Yu
Institute of Urban Environment Chinese Academy of Sciences
Yin Wang (yinwang@iue.ac.cn)
Institute of Urban Environment Chinese Academy of Sciences

Research Article

Keywords: Mercaptans removal, Gasoline oil, Adsorption, Intra-particles space, Core-shell activated carbon

Posted Date: March 30th, 2021

DOI: https://doi.org/10.21203/rs.3.rs-326696/v1

Version of Record: A version of this preprint was published at Environmental Science and Pollution Research on July 10th, 2021. See the published version at https://doi.org/10.1007/s11356-021-15075-y.

Adsorption performance and mechanisms of mercaptans removal from gasoline oil using core-shell AC-based adsorbents: Role of intra-particles space

Pamphile Ndagijimana[a], Xuejiao Liu[a,*], Zhiwei Li[a], Zhenjiao Xing[a], Beibei Pan[a], Guangwei Yu[a], Yin Wang[a,*]

[a]CAS Key Laboratory of Urban Pollutant Conversion, Institute of Urban Environment, Chinese Academy of Sciences, Xiamen 361021, China

[*]Corresponding authors. E-mail address: yinwang@iue.ac.cn (Y. Wang), xjliu@iue.ac.cn (X.J. Liu)

Abstract

Sulfur compound detection such as mercaptans in liquid fuels is undesirable because sulfur is the main sourcing emission of sulfur oxide (SO_x) into the air. The use of activated carbon (AC) has proven to efficiently remove mercaptans. In the meantime, it is limited by the generation of the second pollution in oil, and the difficulties of recovery and regeneration. To address these issues, a core-shell structured AC with high mechanical strength and big intra-particles space were synthesized and demonstrated to efficiently remove organic pollutants from an aqueous solution without generation of the second pollution in our previous work. However, the performance, characteristics, and mechanism of mercaptans adsorption from gasoline oil by core-shell structured AC was still unclear. In this study, the mercaptans adsorption behaviors using core-shell powdered activated carbon (CSAC) and core-shell granulated activated carbon (CSGAC), along with raw PAC, PAC-core, raw GAC, and GAC-core were carried out. The results showed that both the CSAC and CSGAC adsorbents effectively removed sulfur-based pollutants and were provided with good recovery and recyclability without second pollution in gasoline oil. The CSGAC exhibited a higher mercaptans removal efficiency compared to those of CSAC as a result of the bigger intra-particles space. PAC-based adsorbents, presented the shrinking of removal efficiency after regeneration. The Pseudo-second-order kinetics and Langmuir isotherms models were dominated for mercaptans adsorption by both CSAC and CSGAC. Furthermore, the interactions between mercaptans and the composites were probably ascribed to the Van der Waals force, hydrophobic compatibility, pore texture, and π-π dispersion interaction.

Keywords: Mercaptans removal, Gasoline oil, Adsorption, Intra-particles space, Core-shell activated carbon

1. Introduction

The most common and biggest source of energy in the world is from fossil fuels and crude oil. The main parts of crude oil include gasoline, diesel, and jet fuel, which are used as transportation fuels (Srivastava, 2012). The use of liquid fuels (gasoline, diesel, kerosene, jet fuel, etc.) in industrial, transport, and domestic activities for energy production constitute an important source of air pollution (Fan et al., 2013; Shen et al., 2009). However, when using these fuels, the release of persistent impurities, especially for small organic sulfur compounds (mercaptans, thioethers, disulfides, and others) is still an issue that is raising concern (Daraee et al., 2021; Mahmoudabadi, 2021; Sun et al., 2017). Mercaptans (thiol) are featured by unbearable odor as a result of sulfur-contained compounds (Bashkova et al., 2002). They are the most harmful sulfur-carry compounds in gasoline, not only due to their unpleasant-smell and corroding (Gao et al., 2009; Zhang et al., 2013) but also to the degrading gasoline quality by enhancing the production of gum (Wang et al., 2014). The sulfur compounds in gasoline could generate pollution in the environment because their combustion emits sulfur dioxide in the atmosphere, which generates acid rain leading to environmental hazards (Daraee et al., 2021; Mguni et al., 2019; Mohebbi and Mohebbi, 2017).

The removal of mercaptans from fuel has been a global challenge. Various technologies such as adsorption, extraction, bioprocesses, and oxidation for reducing the sulfur compound from fuel are introduced (Dehghan and Anbia, 2017; Rodríguez-Cabo et al., 2014; Wang et al., 2014). For example, the hydrodesulfurization technique could treat such pollutants, but it reduces the octane number of gasoline (Wang et al., 2014), leading to the degradation of the quality of the resultant gasoline product (Huang et al., 2018). High temperature and pressure are also required in this technique (Farzin Nejad and Miran Beigi, 2015). Catalytic oxidation is another limitation for other techniques due to the conversion of mercaptans disulfides in alkaline media through oxidation with air (Koncsag and Barbulescu, 2008; Rodríguez-Cabo et al., 2014; Shiraishi et al., 2002). It has been reported that the adsorption is effective for mercaptans removal from gasoline (Aguiar and Coelho, 2017; Mguni et al., 2019) resulting from its affordable operations and environmental-friendliness. Activated carbon (AC) is a popular adsorbent in removing the mercaptans

(Bashkova et al., 2002; Mguni et al., 2019), which is considered as a good adsorbent in pollutant control (Lee et al., 2010). However, the limitations such as difficulty to recovery from the liquid phase, causing the second pollution in the liquid phase, and low recyclability are the main challenges of using AC in the adsorption process. To address these issues, our group synthesized novel recyclable AC materials (core-shell structured powdered and granulated AC, i.e., CSAC and CSGAC) recently. The results indicated that pharmaceuticals and personal care products (PPCPs) could be efficiently removed from an aqueous solution by these composites (Ndagijimana et al., 2020, 2019a, 2019b). In the meantime, the material further presented a good regeneration and recover-ability. Nonetheless, our previous studies focused on the organic pollutants in the aquatic phase rather than the mercaptans in organic solvents, which probably results in different adsorption behaviors and mechanisms. In addition, comparisons of mercaptans adsorption by CSAC and CSGAC were not carried out. Accordingly, to support the real implementations of core-shell AC composites, it is indispensable to disclose the mercaptans adsorption behaviors from an organic solvent by CSAC and CSGAC, as well as to depict the influence of core-shell AC with AC core produced by AC in different particle size. It is equally important to evaluate the performance of regeneration and recover-ability of CSAC and CSGAC in an organic solvent.

Therefore, based on the previous studies (Ndagijimana et al., 2020, 2019a, 2019b), the objectives of this work were as follows: (i) to compare the performance of CSAC, CSGAC, PAC, PAC-core, GAC, and GAC-core in adsorbing mercaptans; (ii) to evaluate and compare the regeneration and recover-ability of CSAC, CSGAC, PAC, PAC-core, GAC, and GAC-core; (iii) to explore interaction mechanisms via investigating the adsorption kinetics, isotherms, and surface composition of adsorbents before and after adsorption; (iv) to test effects of coexisting mercaptans on the adsorption performance. This work is expected to be in favor of providing an effective strategy for mercaptans' removal from fuel.

2. Materials and methods

2.1. Chemicals and reagents

The n-hexane was used as the solvent. The sulfur compounds were purchased from Aldrich, including ethyl-mercaptan, propanethiol, and 1-butanethiol with a purity of 98, 98, and 99%, respectively. Table 1 presents the structure and physicochemical properties of mercaptans.

2.2. Preparation and characterization

As described in our recent works (Ndagijimana et al., 2020, 2019a, 2019b), the PAC-core and GAC-core were prepared by mixing the PAC (100 mesh) and GAC (2 mm) with 8% and 15% of natural binder from cassava, respectively. As for the shell, coal fly ash with 100 mesh and kaolinite with 400 mesh were selected owing to the formation of CSAC with small intra-particles space in the shell to protect PAC from degeneration (Ndagijimana et al., 2019a, 2019b), whereas, the coal fly ash with 100 mesh and 100 mesh of kaolinite were selected to the synthesize CSGAC with large porous channels (Ndagijimana et al., 2020). The AC-core after drying was coated by the mixture of kaolinite and cola fly ash as the shell. The samples were dried and then sintered at 1250^{o}C followed by cooling at room temperature. Thereafter, the samples were characterized by the ZL-8001 computer servo universal material testing machine (China). The materials with high mechanical strength (2.41 and 2.0 MPa) were selected and used to remove mercaptans. The morphology and the crystalline were analyzed by field emission scanning electron microscopy (SEM) and X-ray diffraction (XRD), respectively. The surface area, pore size, and pore volume were tested by Brunauer-Emmett-Teller (BET). The details of characterization techniques for AC-based adsorbents were described in a recent report (Ndagijimana et al., 2020, 2019a, 2019b).

2.3. Batch adsorption

The preparation of mercaptans solution was carried out as follows: Firstly, the standard hexane solution containing 1000 ppb mercaptans compound was prepared in the bottles of 100 mL by dissolving the accurate weight of sulfur compounds in n-hexane solvent. Then, the bottles with rubber caps and aluminum rings were used to avoid evaporation and surroundings. This solution prepared for each compound was used to prepare the desired concentration of each sulfur compound.

A batch adsorption study was carried out by using 0.24 g of CSAC, 0.28 g of CSGAC, 0.05 g of PAC-based adsorbents (PAC and PAC-core), and 0.03 g of GAC-based adsorbents (GAC and GAC-core). Each adsorbent was taken into a bottle of 100 mL and then sealed with rubber caps. Then, 50 mL of each sulfide compound solution was introduced into the bottles which contain the adsorbents. The cellulose membrane with 0.45 μm pore size was used for filtration of the supernatant after shaking the bottle samples with a speed of 200 *rpm* at 25^{o}C. Then the supernatant was analyzed by Gas Chromatograph (GC). The detection conditions of GC contain detector (Mass spectrometric detector), oven temperature (45-240^{o}C), injector temperature (220^{o}C), and detector temperature (230^{o}C). The filtrate was proved with Gas Chromatography-Mass Spectrometry systems via an AOC-20i autosampler (Agilent 7890B-Agilent 5977B, Agilent, USA) and with the help of GS-GASPRO capillary column (30m × 320 μm × 0 μm, J&W Scientific Inc, USA) (30m × 320 μm x_0μm). Helium was utilized as the carrier gas and the mobile phase was hexane. The retention time of ethyl mercaptan, 1-propanethiol, and 1-butanethiol were 6, 7, and 9 min, respectively.

Effect of adsorbent dosage: One, two, and three balls of core-shell ACs, 0.03, 0.05, and 0.10 g for both PAC and GAC-based adsorbents were used. The initial concentration of mercaptans was 2000 ppb and the adsorption time was 600 min.

Effect of initial concentration: The initial concentration of 800, 900, 1000, 1200, 1500, and 2000 ppb for each sulfide compound were prepared. The samples were withdrawn at a certain adsorption time.

Effect of contact time: The initial concentration of mercaptans was1000 ppb. The supernatants samples were withdrawn at a certain interval of time.

Effect of temperature: The adsorption experiments were carried out at the temperature of 25, 30, 40, 60^{o}C, respectively. The initial concentration of mercaptans was 1000 ppb.

Regeneration of adsorbents: The spent adsorbents were regenerated at 600^{o}C for further adsorption process.

The amount of adsorption at equilibrium, at time t, and the percentage of mercaptans removal were calculated via equations (1), (2), and (3), respectively.

$$q_e = \frac{(c_o - c_e)\times V}{M} \quad (1)$$

$$q_t = \frac{(C_0 - C_t)\times V}{M} \quad (2)$$

$$R = \frac{(C_o - C_e)\times 100}{C_o} \quad (3)$$

where $q_{e\ and}$ q_t (mgS g^{-1}) are the adsorption capacity at equilibrium and time t, R (%) is the removal percentage, and C_0 and C_e are the liquid-phase concentrations of mercaptans at initial time and equilibrium, respectively. V (L) is the volume of the solution and M (g) is the mass of the CSAC.

2.4. Adsorption isotherms and kinetics

The capacity of mercaptans adsorption and isotherms parameters were calculated in virtue of the adsorption isotherms model. The details for the calculation of the isotherm parameters were presented in studies (Barzamini et al., 2014).

The Langmuir model and Freundlich isotherm are expressed as follows: equation (4) and (5):

$$\frac{C_e}{q_e} = \frac{1}{K_L q_m} + \frac{C_e}{q_m} \quad (4)$$

$$\ln q_e = \ln k_F + \left(\frac{1}{n}\right) \ln Ce \quad (5)$$

The corresponding introductions of the parameters were found in lots of studies (Ndagijimana et al., 2019a). For further studying the adsorption characteristics, three kinetics models were applied, including pseudo-first-order, pseudo-second-order, and intra-particle models. The equations (6), (7), and (8) below were applied to fit the kinetics data.

Pseudo-first order model: $\ln (q_e - q_t) = \ln q_t - k_1 t$ (6)

Pseudo-second order model: $\frac{t}{q_t} = \frac{1}{k_2 q_e^2} + \frac{t}{q_e}$ (7)

Intraparticle diffusion: $q_t = k_{dif} t^{1/2} + C$ (8)

Similarly, the introductions of the corresponding parameters were described in the study (Liu et al., 2019).

3. Results and Discussion

3.1. Characterizations

The physical image, the morphological information of CSAC, and its core and shell are presented in Fig.1. Fig. 1a shows that the shell of the materials is porous, and favorable for adsorbate solution to diffuse

166 to the inner AC core. For Fig. 1b as explained in previous work (Ndagijimana et al., 2019b), after
167 optimization of the shell particle size, the inter-particles space of the shell was small to prevent the PAC
168 core from release of the part of PAC to the solution. In addition, Fig. 1c illustrates that the shell with larger
169 inter-particles space is favorable for the protection of GAC and simultaneously facilitates the high rate of
170 mass diffusion which is good evidence for increasing removal efficiency for CSGAC. Figs. 1d-g present
171 the physical images of the CSAC, CSGAC, GAC-core, and PAC-core, respectively. As shown in the figure,
172 the GAC-core presented the larger intra-particles space compared to that of PAC, which is owing to the
173 larger size in GAC (2 mm). Figs. 1h and I show that the pore structure of the PAC core and GAC core after
174 the sintering and the detail is illustrated in our recently reported work (Ndagijimana et al., 2020). The
175 structure of the materials indicates the presence of pores which is beneficial for the adsorption of the
176 aforementioned pollutants in gasoline oil.

177 The textural structure such as specific surface area calculated by BET equation (S_{BET}) and pore
178 distribution of the samples was analyzed and presented in Table 2 and Fig. 2, respectively. As illustrated in
179 Table 2, the CSAC presented a higher S_{BET} compared to that of CSGAC. Moreover, S_{BET} of the PAC-core
180 and GAC-core detached from shell were higher than those of PAC and GAC, respectively, because of
181 sintering of the sample at high temperature (1250^{o}C). Fig. 2 illustrates the presence of pore distribution and
182 pore size of AC-based adsorbents. It evidences the presence of micropores and mesopores for all AC-based
183 adsorbents (Figs. 2a and b), and macropores especially for CSGAC (Figs. 2c and d). The macropores
184 facilitate the penetration of the adsorbate molecular from the bulk solution to the shell and then to the inner
185 core.

186 *3.2. Application for mercaptans removal*

187 *3.2.1. Effect of adsorbent dosage*

188 One, two, and three balls of CSAC and CSGAC were used to investigate the influence of adsorbent
189 dosage (Fig. 3a). As shown in the figure, the removal efficiency of mercaptans and the dosage of adsorbents
190 were positively correlated. For instance, the removal efficiency was 33, 67, and 100% for ethanethiol and
191 28, 54, and 81% for 1-Butanethiol by CSAC, respectively. Furthermore, 98, 100, and 100% of ethanethiol

192 and 41, 75, and 100% of 1-Butanethiol were removed by CSGAC, respectively. These results presented
193 that both the removal efficiencies for ethanethiol and 1-butanethiol by CSGAC were higher than that of
194 CSAC. This phenomenon is caused by the large intra-particles space in the shell and GAC-core for CSGAC.
195 These intra-particles space could facilitate contact between mercaptans molecular and active sites of GAC-
196 core inside the shell. Despite a low removal mercaptans efficiency by CSAC, it should be noted that as-
197 synthesized protected AC materials showed a promising future for removing mercaptans from the gasoline
198 oil. As illustrated in Figs. 3b and c, the dosages used in this experiment were 0.03, 0.05, and 0.10 g for
199 PAC, PAC-core, GAC, and GAC-core, respectively. The results also showed that the removal efficiency
200 increased with adding more adsorbents as a result of more active sites. In addition, the performance of
201 mercaptans adsorption by PAC-core and GAC-core were better than those of their counterparts (PAC and
202 GAC). This phenomenon is likely due to the higher S_{BET} after sintering treatment at high temperatures.
203 Accordingly, the large intra-particles space in shell and AC-core and high S_{BET} are key factors enhancing
204 the adsorption of mercaptans using CSGAC.
205 *3.2.2. Effect of contact time*
206 The effect of contact time on mercaptan adsorption is shown in Fig. 4. It is observed from Figs. 4a and
207 b that the equilibrium of ethanethiol adsorption attained within 420-480 min and 600 min for CSGAC and
208 CSAC, respectively. The results demonstrate a faster adsorption rate of ethanethiol on CSGAC compared
209 to that of CSAC. Concerning the 1-butanethiol, the adsorption equilibrium reached 720 min for CSAC and
210 around 540-600 min for CSGAC, respectively. This phenomenon similarly indicates a higher removal
211 efficiency of mercaptans using CSGAC. These outcomes could be resulted from the large porous channels
212 in a shell for CSGAC and in GAC-core. Furthermore, the removal rate of 1-butanethiol is slower than
213 ethanethiol by both adsorbents, which is likely due to the short-chain of ethanethiol molecular. This was
214 evidenced by (Barzamini et al., 2014), that the adsorption of mercaptans with long-chain would take a
215 longer time to enter into the pore of the adsorbent. Figs. 4b and c illustrate the ethanethiol and 1-butanethiol
216 adsorption by PAC and PAC-core. As depicted in the figures, the equilibrium time for adsorption of these
217 two kinds of mercaptans by PAC and PAC-core is shorter than adsorption by CSAC. Moreover, in

comparison to the adsorption rate of the ethanethiol and 1-butanethiol using PAC, the value by PAC-core is slower. Likewise, the descending order of the mercaptans adsorption rate was GAC, GAC-core, and CSGAC (Figs. 4e and f). This phenomenon could be explained by the mass transfer of ethanethiol and 1-butanethiol molecular from the liquid phase to active sites of the AC-based adsorbents. With regards to the CSAC or CSGAC, the shell would obstacle the mass transfer of molecules from the bulk solution to the surface of adsorbents. Furthermore, the time for ethanethiol adsorption is shorter compared to that of the 1-butanethiol. This outcome is attributed to the short-chain in ethanethiol as mentioned above, which is beneficial for effective mass transfer. Nonetheless, mechanical strength is still an important issue to guarantee real implementations of AC.

The kinetic parameters are shown in Table 3 and Table S1. According to the data, both the pseudo-first-order and pseudo-second-order models are dominated on adsorption of ethanethiol by CSAC. Nevertheless, the pseudo-second-order kinetic model describes better the sorption of ethanethiol by CSGAC. With regards to 1-butanethiol, the pseudo-second-order kinetic model is better fitted to adsorption processes by CSAC and CSGAC. According to the data of R^2 in Table S1, the pseudo-second-order models are dominated on adsorption of the mercaptans by PAC, PAC-core, GAC, and GAC-core. The intra-particle diffusion is used to determine the diffusion process. According to the R^2 values, the adsorption process is not controlled by intra-particle diffusion.

3.2.3. Effect of initial concentration

Fig. 5 and Fig. S1 illustrate the effect of the initial concentration on the mercaptans adsorption by the AC-based adsorbents. Figs. 5a and b show adsorption of the ethanethiol and 1-butanethiol by CSAC and CSGAC under different initial concentrations, respectively. It can be seen from the figures that the adsorption amount of the ethanethiol and 1-butanethiol increased as to increase the initial concentration. The figures also illustrated that the removal efficiency for CSGAC is still higher compared to that of CSAC. This phenomenon is attributed to the large intra-particles space in the shell and GAC-core for CSGAC. As shown in Fig. S1, the ethanethiol and 1-butanethiol adsorption by PAC, GAC, PAC-core, and GAC-core depicted similar trends with that of CSCA and CSGAC. This result is probably owing to the limited number

of active sites on a constant amount of the adsorbents. Furthermore, adsorption isotherms of the ethanethiol and 1-butanethiol by CSAC and CSGAC were better fitted to the Langmuir model (Fig. 5c). The q_m and k_L are calculated according to the slope and intercept of a linear plot of C_e/q_e against C_e, where the slope is corresponding to $1/q_m$ and intercept equals to $1/q_mk_L$. The corresponding parameters were shown in Table 4. Likewise, the ethanethiol and 1-butanethiol adsorption using PAC, GAC, PAC-core, and GAC-core were also better fitted to the Langmuir model (Table S1). This outcome indicates that the ethanethiol and 1-butanethiol were removed by all of the AC-based adsorbents via monolayer adsorption. Accordingly, the ethanethiol and 1-butanethiol adsorption characteristics by CSAC and CSGAC were not changed after being protected by the shell. Furthermore, the adsorption capacities of ethanethiol and 1-butanethiol by CSAC were 139.28 and 125.63 μgS g^{-1}, respectively. And adsorption capacities of ethanethiol and 1-butanethiol by CSGAC were 190.48 and 151.52 μgS g^{-1}, respectively. Additionally, 100 and 100%, and 97.24 and 74.29% of ethanethiol and 1-butanethiol were removed by GAC-core and GAC, respectively. Hence, ethanethiol is more efficiently adsorbed compared to 1-butanethiol by the adsorbents. This is likely ascribed to the smaller resistance of mass transfer from shell to the surface of the AC core for short-chain ethanethiol. Furthermore, CSGAC exhibits a better adsorption performance to ethanethiol and 1-butanethiol than that of CSAC. This could have resulted from the larger intra-particles space of the shell and GAC core which is feasible for mercaptans molecular arriving at the GAC core and entrancing inner core. What's more, despite a better performance of the mercaptans removal using non-protected AC, the protected AC (CSAC and CSGAC) presented future promising of a good adsorbent for mercaptans removal from gasoline oil due to their good recovering and recycling.

3.2.4. Influence of temperature and thermodynamic study

The adsorption of ethanethiol and 1-butanethiol in the case of temperatures of 25, 30, 40, and 60°C were further investigated (Fig. 6 and Fig. S2). It can be seen from the figures that the adsorption capacities of ethanethiol and 1-butanethiol by most of the AC-based adsorbents increased as temperature increased. This phenomenon is likely due to a decrease of the viscosity of the adsorbate solution as an increase in temperature, leading to the improvement of the diffusion rate of adsorbate molecular through the external

boundary layer to the internal pores of adsorbents (Meshkat et al., 2018a, 2018b). The results demonstrate that q_m increases as temperature elevates (Table 5), suggesting that a higher temperature promotes the removal of mercaptans.

To better understand the effects of temperature, the thermodynamic parameters (Meshkat et al., 2018a, 2018b) were evaluated by Van't Hoff equations:

$$\ln\left(\frac{q_e}{C_e}\right) = -\frac{\Delta H^\circ}{RT} + \frac{\Delta S^\circ}{R} \quad (9)$$

$$(\Delta G^\circ) = \Delta H^\circ - T(\Delta S^\circ) \quad (10)$$

where and T are presenting the universal gas constant (8.314 J mol^{-1} K^{-1}) and the absolute temperature. Plotting ln (q_e/C_e) versus 1/T shows a linear line with slope and intercept similar to -ΔH°/R and ΔS°/R, respectively (Figs. 7a-d).

The positive value of ΔH° in Table 6, Table S3, and Table S4 indicate that ethanethiol and 1-butanethiol adsorption by CSAC, CSGAC, PAC-core, GAC, and GAC-core are endothermic processes. The data for PAC, PAC-core, GAC, and GAC-core were presented in supporting information Table S3 and Table S4. The negative value of ΔH° (Table S3) for PAC indicates that the process is exothermic. The Gibb free energy of adsorption (ΔG°) is estimated via Eq. 10. This negative data shows evidence of a spontaneous adsorption reaction between adsorbents and ethanethiol and 1-butanethiol molecular. It is observed that the heat from the physical adsorption falls into a range of 2.10-20.9 kJ mol^{-1}, while the heat of chemisorption locates at a range of 80-200 kJ mol^{-1}. Both values are consistent with those of previous studies (Meshkat et al., 2018a, 2018b).

3.3. Adsorption competition

Except for the ethanethiol and 1-butanethiol, 1-propanethiol was used as a coexisting organics to investigate adsorption competence between these molecular by CSAC and CSGAC. In this study, the solution of ethanethiol, 1-propanethiol, and 1-butanethiol with a concentration of 1000 ppb in a bottle of 100 mL was used to investigate the capability of the material in the competition of adsorption to different kinds of mercaptans. Fig. 8 depicts that the ethanethiol is highly adsorbed while the 1-butanethiol is weakly

295 removed by CSAC and CSGAC adsorbents, which is resulted from the short-chain of ethanethiol. The
296 competition effect also was performed on PAC-based adsorbents and GAC-based adsorbents, the results
297 showed that ethanethiol is still highly removed compare to others and slightly affected by the competition
298 (Fig. 8). The reason is the same as mentioned above. For PAC-core and GAC-core presented high removal
299 efficiency for all adsorbents during the competition. This is attributed to the high active site generated to
300 the sintering of the sample at high temperatures. Conclusively, the increasing of the adsorption of
301 mercaptans in multi pollutants environment will depend on the small molecular chain of mercaptans, the
302 large intra-particles space of core-shell ACs, and high S_{BET}.

303 *3.4. The regeneration of CSGAC*

304 The regeneration process after the removal of mercaptans from gasoline oil was evaluated to confirm
305 its re-usage and recyclability after the adsorption. As shown in Fig. 9a, the regenerated adsorbents still
306 illustrate almost the same adsorption performance after regeneration of exhausted adsorbents six times.
307 This result reveals a good regeneration performance and high stability of the CSGAC for mercaptans
308 removal. Fig. 9b shows that the removal efficiency of PAC highly decreases after the regeneration at the
309 fourth time compared to that of PAC-core. This is likely due to the more difficult recovering process
310 compared to that of PAC-core. GAC-based adsorbents (GAC and GAC-core) showed a slightly shrinking
311 of mercaptans removal (Fig. 9c) compared to the PAC-based adsorbents. GAC-based adsorbents are easily
312 recovered and also the small amount lost during recovering and recycling. In all, the original AC-based
313 adsorbents and AC-core (PAC-core and GAC-core) presented a shrinking removal efficiency, whereas, the
314 protected activated carbon-based adsorbents (CSAC and CSGAC) presented the constant removal
315 efficiency after six times of regeneration. This outcome evidences a promising application of protected
316 activated carbon-based adsorbents for mercaptans removal from the gasoline oil.

317 *3.5. The possible mechanisms of mercaptans adsorption by CSACs*

318 As illustrated in the previous study, the pore structure is a crucial factor to determine the mechanisms
319 of adsorption of organic matter. As can be seen from Fig. 1, it is obvious that the material is provided with
320 an apparent porous structure. Owing to this property, mercaptan molecular from bulk solution goes across

the shell to the external surface of the AC core and then continues to the inner core. As for CSGAC, features such as the large intra-particles space between shell particles (Fig. 1c), broken pore structure (Fig. 1I), an increasing of S_{BET}, micropore, and mesopores volumes of AC core after sintering at 1250°C (Table 2), are advantageous for the removal of mercaptans into the pores of the GAC core.

Fig. 10 shows the TGA diagrams on saturated CSAC with mercaptans. Generally, the curves show an initial weight loss in the temperature range of 40-200°C, which is the degradation of adsorbed mercaptans and impurities. This phenomenon indicates clearly that mercaptans are fixed in the adsorbents. The mass loss of the adsorbent is very insignificant because the adsorbents are sintered at high temperatures (Meshkat et al., 2018a, 2018b).

Besides, the adsorption of ethanethiol and 1-butanethiol on CSAC or CSGAC was further confirmed by elemental analysis (Table 7). As shown in the table, the number of sulfur increased after the adsorption of sulfide compounds on core-shell AC adsorbents. These results further prove the existence of mercaptan molecular on the surface of adsorbents surface.

Furthermore, the FTIR analysis (Fig. 11) was performed to detect the adsorption of mercaptans by CSACs. According to the previous work (Cheng et al., 2020; Meshkat et al., 2018b; Pham et al., 2013), the new peaks between 1155 to 600 cm^{-1} could be corresponding to the bond between C and S. Although no new peak appeared after adsorption of ethanethiol on CSGAC, the result indicates the appearance of the new peaks after adsorption of 1-butanethiol and ethanethiol by CSAC and CSGAC.

Conclusively, the results provided by TG, elemental analysis, and FTIR after adsorption, consistently state clear that the mercaptans molecular are adsorbed on the core-shell structured AC composites. The Van der Waals forces, electron donor-acceptor interactions, and chemical affinity are responsible for the adsorption of the mercaptans (Dehghan and Anbia, 2017). The high mercaptan removal efficiency of adsorbent requires a large size and high dipole moment of mercaptan, which is attracted to adsorbent with strong Van der Waals (Meshkat et al., 2018b). The electron donor-acceptor interactions between the S atoms and the basic adsorbent, the dispersion effect between the mercaptans molecular and the π-electrons of the carbon adsorbent are two important factors. The energetic heterogeneity is caused by the connectivity,

shape, and number of structures (Meshkat et al., 2018b). In virtue of the optimal pore texture and forces such as the Van der Waals force, π-π dispersion interaction, and hydrophobic compatibility of mercaptans molecular with the surface of the adsorbent, mercaptans molecular could be efficiently removed from the fuel.

4. Conclusions

The mercaptans from the gasoline oil are efficiently removed by core-shell AC-based Adsorbents (CSAC and CSGAC). The protected ACs are future good adsorbent as presented the good recovering and recycling after adsorption of mercaptans. The large intra-particles space in both the shell and AC are advantageous of good adsorption performance of CSGAC compared to that of CSAC. Although the PAC, PAC-core, and GAC-core presented high performance compared to their protected forms, their adsorption capacity was shrunk after the regeneration due to their low recovering and recycling after adsorption. The mercaptan adsorption by core-shell AC adsorbents was more precisely fitted to Langmuir isotherm than the Freundlich model. The capacity of Ethanethiol and 1-Butanethiol by CSGAC adsorption are 190.48 and 151.52 μgS g^{-1}, respectively. The mercaptan adsorption by core-shell AC adsorbents is proven to be an endothermic and spontaneous process. The core-shell AC materials are also proved with good recyclability and regeneration at 600^{o}C. The possible mechanisms of the adsorption on CSGAC simultaneously depend on Vander Waal's force, pore texture, π-π dispersion interaction, and hydrophobic properties of mercaptan molecules.

Acknowledgments

The Authors acknowledged, the Strategic Priority Research Program of the Chinese Academy of Sciences [Grant No. XDA23030301, XDA23020504], the Special Research Assistant Program of the Chinese Academy of Sciences, the Science and Technology program of Xiamen (Grant No. 3502Z20203075, 3502Z20203074), as well as CAS-TWAS President's Fellowship Program.

Ethical Approval

This manuscript is original not submitted to other journals nor published elsewhere. The work was not split into many parts presented, and there is no fabrication, falsification or inappropriate data manipulation. This work has no plagiarism, and the similarities have been decreased to under 25% and proper acknowledgement was given.

Consent to Participate

All authors participated in this work as shown in the statement of Authors contribution.

Consent to Publish

All Authors confirmed that the work has not been published before and it is not under consideration for publication elsewhere.

Authors Contributions

Pamphile Ndagijimana, his contribution focused on doing experiment and writing the manuscript.

Xuejiao Liu contributed in guiding, revising the manuscript and funding the work.

Zhiwei Li, Zhenjiao Xing, Beibei Pan, and Guangwei Yu revised this manuscript.

Yin Wang also contributed in guiding, revising the manuscript and funding the work.

Funding

This work was funded by the Strategic Priority Research Program of the Chinese Academy of Sciences [Grant No. XDA23030301, XDA23020504], the Special Research Assistant Program of the Chinese Academy of Sciences, and the Science and Technology program of Xiamen (Grant No. 3502Z20203075, 3502Z20203074), as well as CAS-TWAS President's Fellowship Program.

Competing Interests

All authors declared that this work has no conflict of Interest.

Availability of data and materials

Regarding the data and material in this manuscript, all authors concluded that, the data available online (DOI link provided by Journal after publication) will be shared according to the requirement of this Journal.

References

Aguiar M F de, Coelho GLV (2017) Adsorption of sulfur compounds from natural gas by different adsorbents and desorption using supercritical CO_2. J. Environ. Chem. Eng. 5, 4353–4364. https://doi.org/https://doi.org/10.1016/j.jece.2017.07.079

Barzamini R, Falamaki C, Mahmoudi R (2014) Adsorption of ethyl, iso-propyl, n-butyl, and iso-butyl mercaptans on AgX zeolite: Equilibrium and kinetic study. Fuel 130, 46–53. https://doi.org/https://doi.org/10.1016/j.fuel.2014.04.013

Bashkova S, Bagreev A, Bandosz TJ (2002) Adsorption of Methyl Mercaptan on Activated Carbons. Environ. Sci. \& Technol. 36, 2777–2782. https://doi.org/10.1021/es011416v

Cheng L, Guan K, Liu G, Jin W (2020) Cysteamine-crosslinked graphene oxide membrane with enhanced hydrogen separation property. J. Memb. Sci. 595, 117568. https://doi.org/https://doi.org/10.1016/j.memsci.2019.117568

Daraee M, Saeedirad R, Ghasemy E, Rashidi A (2021) N-CNT/ZIF-8 nano-adsorbent for adsorptive desulfurization of the liquid streams: Experimental and. J. Environ. Chem. Eng. 9, 104806. https://doi.org/https://doi.org/10.1016/j.jece.2020.104806

Dehghan R, Anbia M (2017) Zeolites for adsorptive desulfurization from fuels: A review. Fuel Process. Technol. 167, 99–116. https://doi.org/https://doi.org/10.1016/j.fuproc.2017.06.015

Fan Y, Shi G, Bao X (2013) A process for producing ultraclean gasoline by coupling efficient hydrodesulfurization and directional olefin conversion. AIChE J. 59, 571–581. https://doi.org/https://doi.org/10.1002/aic.13832

Farzin Nejad N, Miran Beigi A A (2015) Efficient desulfurization of gasoline fuel using ionic liquid extraction as a complementary process to adsorptive desulfurization. Pet. Sci. 12, 330–339. https://doi.org/10.1007/s12182-015-0020-2

Gao L, Xue Q, Liu Y, Lu Y, (2009) Base-free catalytic aerobic oxidation of mercaptans for gasoline sweetening over HTLcs-derived CuZnAl catalyst. AIChE J. 55, 3214–3220. https://doi.org/https://doi.org/10.1002/aic.11928

Huang T, Peng Q, Shi W, Xu J, Fan Y (2018) An anionic surfactant-assisted equilibrium adsorption method to prepare highly dispersed Fe-promoted Ni/Al_2O_3 catalysts for highly selective mercaptan removal. Appl. Catal. B

Environ. 230, 154–164. https://doi.org/https://doi.org/10.1016/j.apcatb.2018.02.053

Koncsag C I, Barbulescu A (2008) Modelling the removal of mercaptans from liquid hydrocarbon streams in structured packing columns. Chem. Eng. Process. Process Intensif. 47, 1717–1725. https://doi.org/https://doi.org/10.1016/j.cep.2007.09.015

Lee S W, Daud W M A W, Lee M G (2010) Adsorption characteristics of methyl mercaptan, dimethyl disulfide, and trimethylamine on coconut-based activated carbons modified with acid and base. J. Ind. Eng. Chem. 16, 973–977. https://doi.org/https://doi.org/10.1016/j.jiec.2010.04.002

Liu X, Lai D, Wang Y (2019) Performance of Pb (II) removal by an activated carbon supported nanoscale zero-valent iron composite at ultralow iron content. J. Hazard. Mater. 361, 37–48. https://doi.org/10.1016/j.jhazmat.2018.08.082

Mahmoudabadi ZS, Tavasoli A, Rashidi A. et al (2021) Catalytic activity of synthesized 2D MoS_2/graphene nanohybrids for the hydrodesulfurization of SRLGO: experimental and DFT study. Environ Sci Pollut Res 28, 5978–5990. https://doi.org/10.1007/s11356-020-10889-8

Meshkat S S, Rashidi A, Tavakoli O (2018a) Removal of mercaptan from natural gas condensate using N-doped carbon nanotube adsorbents: Kinetic and DFT study. J. Nat. Gas Sci. Eng. 55, 288–297. https://doi.org/https://doi.org/10.1016/j.jngse.2018.04.036

Meshkat S S, Tavakoli O, Rashidi A, Esrafili M D (2018b) Adsorptive mercaptan removal of liquid phase using nanoporous graphene: Equilibrium, kinetic study and DFT calculations. Ecotoxicol. Environ. Saf. 165, 533–539. https://doi.org/https://doi.org/10.1016/j.ecoenv.2018.08.110

Mguni L L, Yao Y, Liu X, Yuan Z, Hildebrandt D (2019) Ultra-deep desulphurization of both model and commercial diesel fuels by adsorption method. J. Environ. Chem. Eng. 7, 102957. https://doi.org/https://doi.org/10.1016/j.jece.2019.102957

Mohebbi A, Mohebbi V, (2017) Equilibrium adsorption of ethyl mercaptan and thiophene using molecular sieve 13X. Fluid Phase Equilib. 436, 30–37. https://doi.org/https://doi.org/10.1016/j.fluid.2016.12.023

Ndagijimana P Liu X Li Z, Yu G, Wang Y (2019b) Optimized synthesis of a core-shell structure activated carbon and

its adsorption performance for Bisphenol A. Sci. Total Environ. 689, 457–468. https://doi.org/https://doi.org/10.1016/j.scitotenv.2019.06.235

Ndagijimana P, Liu X, Yu G, Wang Y(2019a) Synthesis of a novel core-shell-structure activated carbon material and its application in sulfamethoxazole adsorption. J. Hazard. Mater. 368, 602–612. https://doi.org/https://doi.org/10.1016/j.jhazmat.2019.01.093

Ndagijimana, P, Liu X, Li Z, Yu G, Wang Y (2020) The synthesis strategy to enhance the performance and cyclic utilization of granulated activated carbon-based sorbent for bisphenol A and triclosan removal. Environ. Sci. Pollut. Res. 27, 15758–15771. https://doi.org/10.1007/s11356-020-08095-7

Pham C V, Eck M, Krueger M (2013) Thiol functionalized reduced graphene oxide as a base material for novel graphene-nanoparticle hybrid composites. Chem. Eng. J. 231, 146–154. https://doi.org/https://doi.org/10.1016/j.cej.2013.07.007

Rodríguez-Cabo B, Rodríguez H, Rodil E, Arce A, Soto A (2014) Extractive and oxidative-extractive desulfurization of fuels with ionic liquids. Fuel 117, 882–889. https://doi.org/https://doi.org/10.1016/j.fuel.2013.10.012

SHEN Y, SHUAI S, WANG J, XIAO J (2009) Optimization of gasoline hydrocarbon compositions for reducing exhaust emissions. J. Environ. Sci. 21, 1208–1213. https://doi.org/https://doi.org/10.1016/S1001-0742(08)62405-5

Shiraishi Y, Tachibana K, Hirai T, Komasawa I (2002) Desulfurization and Denitrogenation Process for Light Oils Based on Chemical Oxidation followed by Liquid−Liquid Extraction. Ind. \& Eng. Chem. Res. 41, 4362–4375. https://doi.org/10.1021/ie010618x

Srivastava VC (2012) An evaluation of desulfurization technologies for sulfur removal from liquid fuels 759–783. https://doi.org/10.1039/c1ra00309g

Sun H, Han X, Liu K, Shen B, Liu J, Wu D, Shi X (2017) Metal-Modified Cu-BTC Acid for Highly Enhanced Adsorption of Organosulfur Species. Ind. \& Eng. Chem. Res. 56, 9541–9550. https://doi.org/10.1021/acs.iecr.7b02392

Wang S, Fan Y, Jia X (2014) Sodium dodecyl sulfate-assisted synthesis of hierarchically porous ZIF-8 particles for

removing mercaptan from gasoline. Chem. Eng. J. 256, 14–22. https://doi.org/https://doi.org/10.1016/j.cej.2014.06.095

Zhang Y, Liu Z, Wang W, Cheng Z, Shen B(2013) Research on the MgO-supported solid-base catalysts aimed at the sweetening of hydrogenated gasoline. Fuel Process. Technol. 115, 63–70. https://doi.org/https://doi.org/10.1016/j.fuproc.2013.03.046

Table 1. Physicochemical properties of mercaptans

Pollutants	Formula	Structure	Water solubility	log K_{ow}	pK_a
Ethanethiol	C_2H_6S	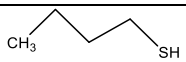	8.86 g/L at 20°C	1.50	10.60
1-Butanethiol	$C_4H_{10}S$	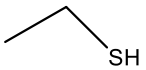	0.06%	2.28	-10.78

513 **Table. 2.** Surface area, pore-volume, and pore size of used carbon-based adsorbents

Sample	Surface area ($m^2 g^{-1}$)	Pore volume ($cm^3 g^{-1}$)	Pore size (nm)
PAC	823.00	0.44	2.15
PAC-core	1095.00	0.59	2.16
CSAC	199.00	0.11	2.50
GAC	509.78	0.28	2.20
GAC-core	978.95	0.54	2.60
CSGAC	141.79	0.06	3.00

514

515

516

517

518

519

520

521

522

523

524

525

526

527

528

Table 3. Kinetics study of Mercaptans adsorption by CSAC and CSGAC

Sorbent	Mercaptans	Pseudo-first-order				Pseudo-second-order				Intraparticle diffusion		
		q_e^{exp} (mg g^{-1})	q_e^{cal} (mg g^{-1})	K_1	R^2	q_e^{exp} (mg g^{-1})	q_e^{cal} (mg g^{-1})	K_2	R^2	C	K_{diff}	R^2
CSAC	Ethanethiol	131.87	94.14	92×10^{-3}	0.99	131.87	137.36	24×10^{-4}	0.99	51.90	3.30	0.83
	1-Butanethiol	116.00	142.68	77×10^{-3}	0.89	116.00	129.00	14×10^{-4}	0.99	4.00	17.86	0.96
CSGAC	Ethanethiol	176.69	138.27	10×10^{-2}	0.98	176.69	184.16	8×10^{-5}	0.99	69.25	4.40	0.84
	1-Butanethiol	135.58	197.44	12×10^{-3}	0.90	135.58	146.41	12×10^{-4}	0.99	31.55	4.20	0.89

529

530

531

532

533

534

535

536

537

Table 4. The isotherm parameters of mercaptans adsorption by CSAC and CSGAC

Sorbents	Sorbates	Langmuir isotherm		
		q_m (μgS g^{-1})	k_L (L mg^{-1})	R^2
CSAC	Ethanethiol	139.28	1.8×10^{-3}	0.999
	1-Butanethiol	125.63	79×10^{-3}	0.998
CSGAC	Ethanethiol	190.48	10×10^{-3}	0.999
	1-Butanethiol	151.52	66×10^{-3}	0.999

538

539

540

541

542

543

544

545

546

547

548

549

550

Table 5. Langmuir parameters as functions of mercaptan molecule and temperature on core-shell ACs

Adsorbents	Mercaptans	Temperature (°C)	q_m (mgS g^{-1})	b (mgS L^{-1})	R^2
CSAC	Ethanethiol	25	139.28	18×10^{-3}	0.999
CSAC	Ethanethiol	30	139.86	17×10^{-3}	0.999
CSAC	Ethanethiol	40	141.84	15×10^{-3}	0.999
CSAC	Ethanethiol	60	142.86	13×10^{-3}	0.999
CSAC	1-Butanethiol	25	125.60	37×10^{-3}	0.998
CSAC	1-Butanethiol	30	128.87	39×10^{-3}	0.999
CSAC	1-Butanethiol	40	132.45	37×10^{-3}	0.999
CSAC	1-Butanethiol	60	135.67	33×10^{-3}	0.999
CSGAC	Ethanethiol	25	190.48	10×10^{-3}	0.999
CSGAC	Ethanethiol	30	196.08	11×10^{-4}	0.999
CSGAC	Ethanethiol	40	202.83	10×10^{-4}	0.999
CSGAC	Ethanethiol	60	206.00	49×10^{-5}	0.999
CSGAC	1-Butanethiol	25	151.5	18×10^{-3}	0.999
CSGAC	1-Butanethiol	30	155.8	19×10^{-3}	0.999
CSGAC	1-Butanethiol	40	157.73	16×10^{-3}	0.999
CSGAC	1-Butanethiol	60	169.21	87×10^{-4}	0.999

561 **Table 6.** Thermodynamic study of core-shell ACs

Adsorbents	Adsorbate	C_0 (mg S L^{-1})	ΔH (kJ mol^{-1})	ΔS (J mol^{-1} K^{-1})	ΔG (kJ mol^{-1})			
					298K	303K	313K	333K
CSAC	Ethanethiol	800	2.37	1.98	1.79	1.78	1.71	1.73
CSAC	Ethanethiol	900	1.44	-2.03	2.04	2.43	2.82	2.11
CSAC	Ethanethiol	1000	3.23	2.04	2.68	2.58	2.51	2.59
CSAC	Ethanethiol	1200	3.92	0.85	3.67	3.65	3.66	3.63
CSAC	Ethanethiol	1500	2.73	-6.35	4.59	4.67	4.76	4.83
CSAC	Ethanethiol	2000	2.99	-9.18	5.69	5.79	5.91	6.03
CSAC	1-Butanethiol	800	3.33	1.41	2.89	2.93	2.91	2.85
CSAC	1-Butanethiol	900	4.05	2.81	3.21	3.24	3.21	3.12
CSAC	1-Butanethiol	1000	3.71	1.32	3.32	3.27	3.35	3.25
CSAC	1-Butanethiol	1200	2.69	-4.78	4.16	4.14	4.13	4.33
CSAC	1-Butanethiol	1500	2.52	-8.52	5.17	5.17	5.13	5.38
CSAC	1-Butanethiol	2000	2.49	-12.16	6.13	6.16	6.28	6.55
CSGAC	Ethanethiol	800	-	-	-	-	-	-
CSGAC	Ethanethiol	900	515.67	1779	-14.4	-23.3	-	-
CSGAC	Ethanethiol	1000	35.27	137.76	-5.4	-7.0	-7.7	-
CSGAC	Ethanethiol	1200	12.93	43.38	0.079	-0.24	-0.73	-1.5
CSGAC	Ethanethiol	1500	8.05	19.41	2.27	2.19	1.93	1.61
CSGAC	Ethanethiol	2000	3.87	0.059	3.93	383	3.76	3.91
CSGAC	1-Butanethiol	800	12.72	39.14	0.91	0.91	0.68	-0.42
CSGAC	1-Butanethiol	900	13.20	39.89	1.14	1.14	1.02	-0.23
CSGAC	1-Butanethiol	1000	12.11	35.41	1.43	1.38	1.27	0.21
CSGAC	1-Butanethiol	1200	12.76	33.09	2.74	2.69	2.50	1.61
CSGAC	1-Butanethiol	1500	8.23	14.09	3.99	3.97	3.86	3.51
CSGAC	1-Butanethiol	2000	4.75	-1.62	5.17	5.16	5.28	5.21

562

563

Table 7. The elemental analysis of pristine and treated CSAC and CSGAC

Elements	N	C	S
CSAC[a]	0.083	12.00	0.041
CSGAC[a]	0.018	11.11	0.042
CSAC[b]	0.055	35.51	0.41
CSGAC[b]	0.044	29.93	0.65

564 [a]Before adsorption

565 [b]After adsorption

566

567

568

569

570

571

572

573

574

575

576

577

578

579

Figures captions

Fig. 1. SEM images of shell (a), intra-particle space or void in shell of CSAC (b), CSGAC (c), physical images of CSAC (d), CSGAC (e), GAC-core (f), PAC-core (g), SEM images of PAC-core (h), and GAC-core (i).

Fig. 2. The pore distribution of PAC-based adsorbent (a), GAC-based adsorbent (b), and core-shell ACs (c, d).

Fig. 3. Effect of adsorbent dosage on the mercaptans removal by CSAC and CSGAC (a), PAC-based adsorbents (b), and GAC-based adsorbents(c). (Conditions: C_0 = 2000 ppm, V = 50 mL, mass = 0.24 g (CSAC), 0.28 g (CSGAC), 0.05 g (PAC-core and PAC), and 0.03 g (GAC-core and GAC)).

Fig. 4. Effect of contact time for CSAC and CSGAC (a, b) and for PAC, PAC-core, GAC, GAC–core (c-f). (Conditions: C_0 = 1000 ppm, V = 50 mL, mass = 0.24 g (CSAC), 0.28 g (CSGAC), 0.05 g (PAC-core and PAC) and 0.03 g (GAC-core and GAC).

Fig. 5. Effect of initial concentration on mercaptans removal (a, b), and Langmuir fitting model (c)

Fig. 6. Temperature effect: Ethanethiol adsorbed on CSAC and CSGAC (a, b), 1-Butanethiol adsorbed on CSAC and CSGAC (c, d).

Fig. 7. The plot of K_C versus 1/T for determination of mercaptans removal reaction enthalpy.

Fig. 8. Adsorption competition of mercaptans by core- shell ACs, PAC-based adsorbents and GAC-based adsorbents. (Conditions: C_0= 1000 ppm, V= 50 mL, mass= 0.24 g (CSAC), 0.28 g (CSGAC), 0.05 g (PAC-core and PAC) and 0.03 g (GAC-core and GAC).

Fig. 9. Thermal regeneration of mercaptans by core-shell AC (a) and PAC and GAC based adsorbents (b, c).

Fig. 10. TG and DTG curves of treated CSAC and CSGAC.

Fig. 11. FTIR spectra of pristine and treated CSAC and CSGAC.

603 **Graphical Abstract**

604

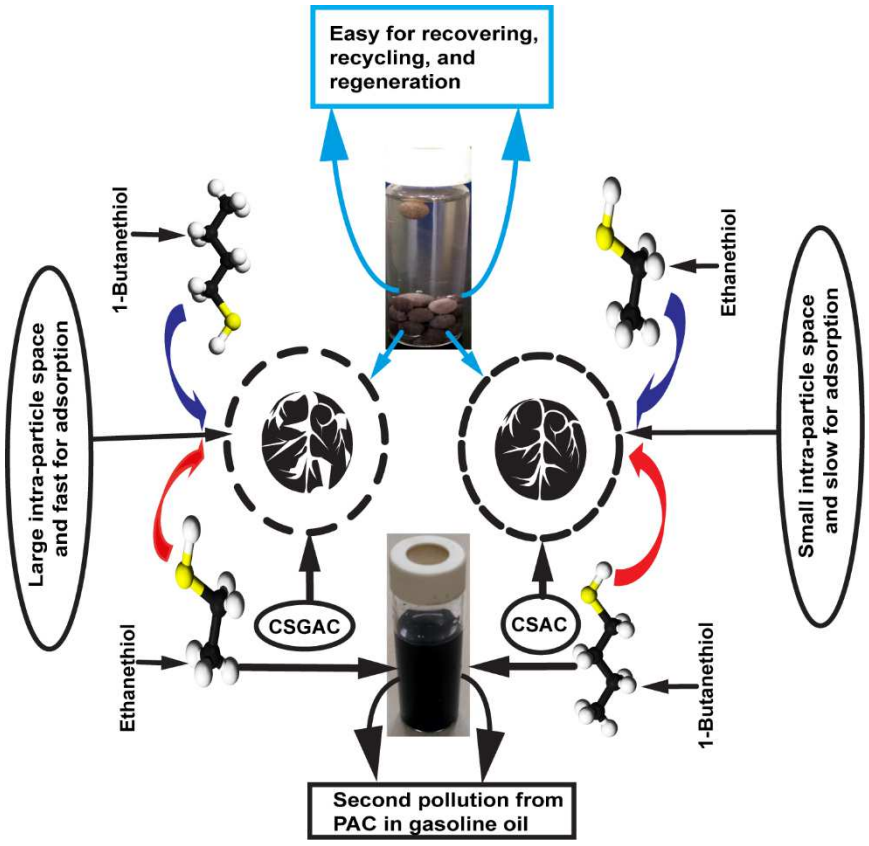

605

606

607

608

609

610

611

612

613

614

615

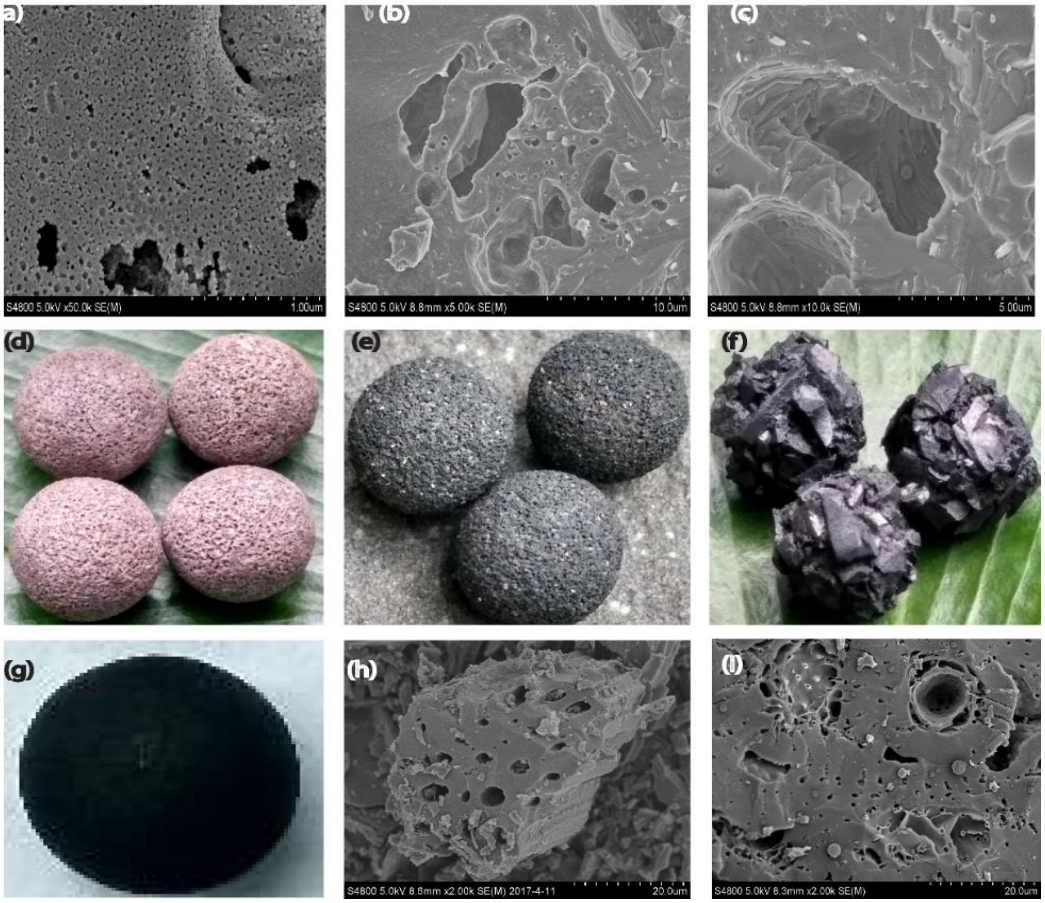
(a)
S4800 5.0kV x50.0k SE(M)
1.00um
(b)
S4800 5.0kV 8.8mm x5.00k SE(M)
10.0um
(c)
S4800 5.0kV 8.8mm x10.0k SE(M)
5.00um
(d)
(e)
(f)
(g)
(h)
S4800 5.0kV 8.8mm x2.00k SE(M) 2017-4-11
20.0um
(i)
S4800 5.0kV 8.3mm x2.00k SE(M)
20.0um

Fig. 1.

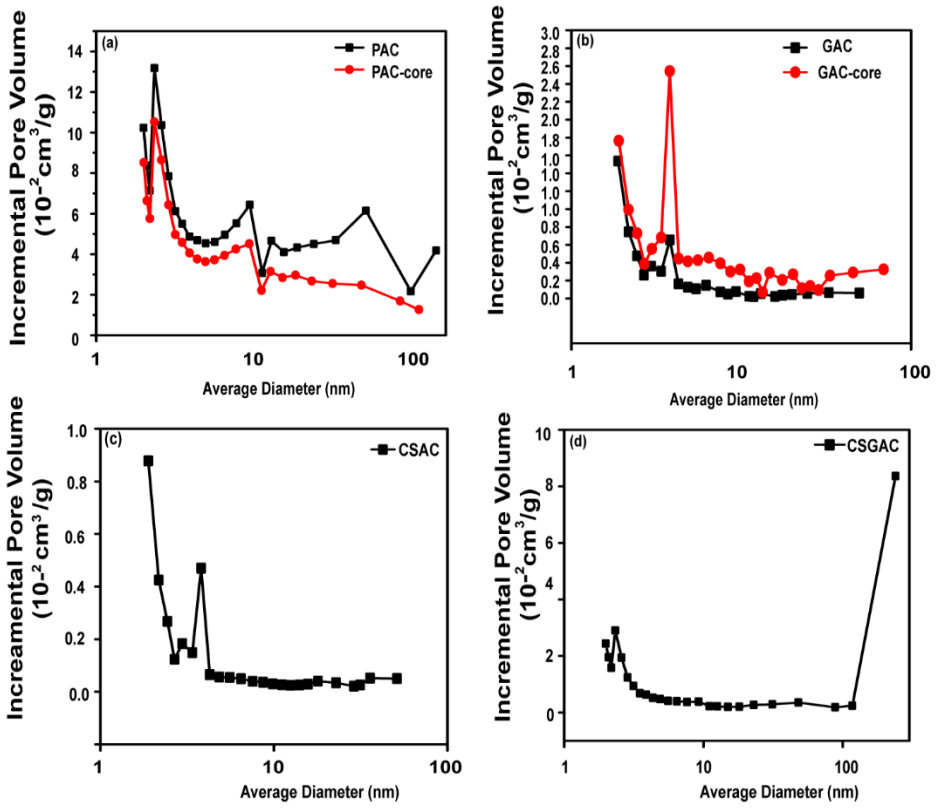

627

628 **Fig. 2.**

629

630

631

632

633

634

635

636

637

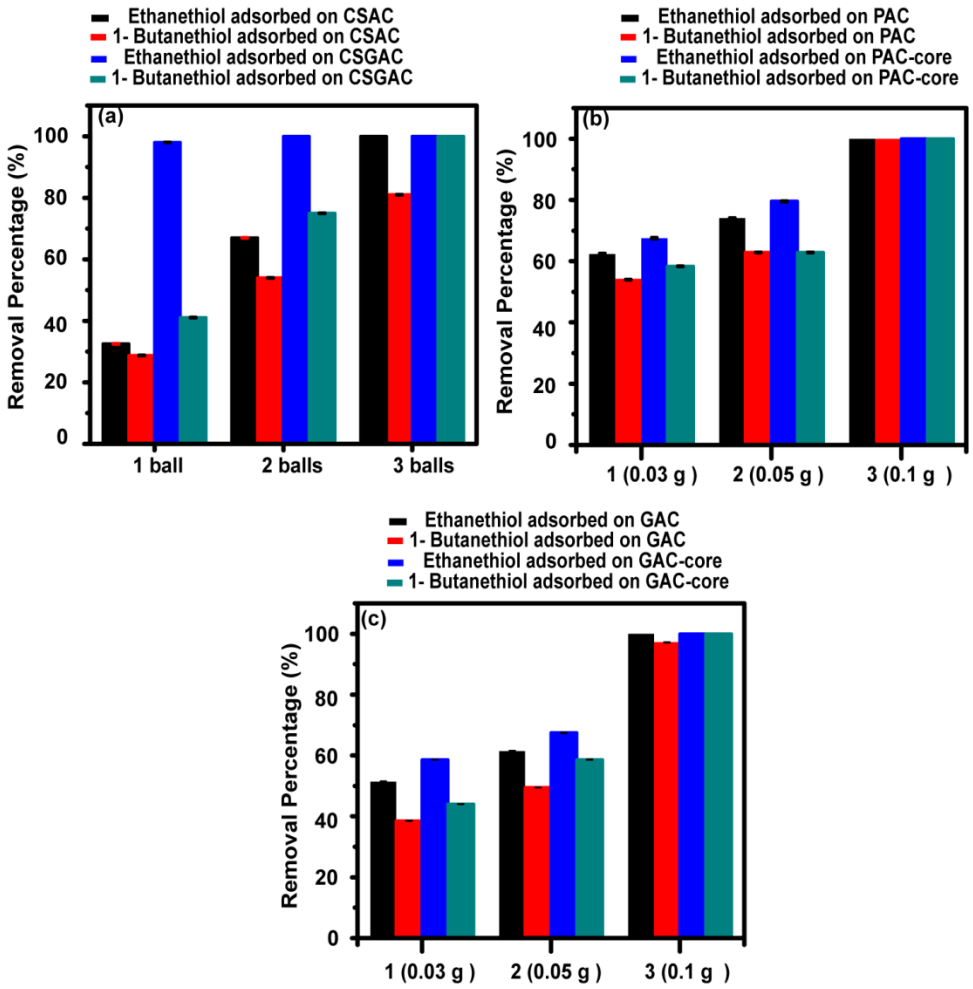
Ethanethiol adsorbed on CSAC
1- Butanethiol adsorbed on CSAC
Ethanethiol adsorbed on CSGAC
1- Butanethiol adsorbed on CSGAC
(a)
Removal Percentage (%)
1 ball
2 balls
3 balls
Ethanethiol adsorbed on PAC
1- Butanethiol adsorbed on PAC
Ethanethiol adsorbed on PAC-core
1- Butanethiol adsorbed on PAC-core
(b)
1 (0.03 g)
2 (0.05 g)
3 (0.1 g)
Ethanethiol adsorbed on GAC
1- Butanethiol adsorbed on GAC
Ethanethiol adsorbed on GAC-core
1- Butanethiol adsorbed on GAC-core
(c)

Fig. 3.

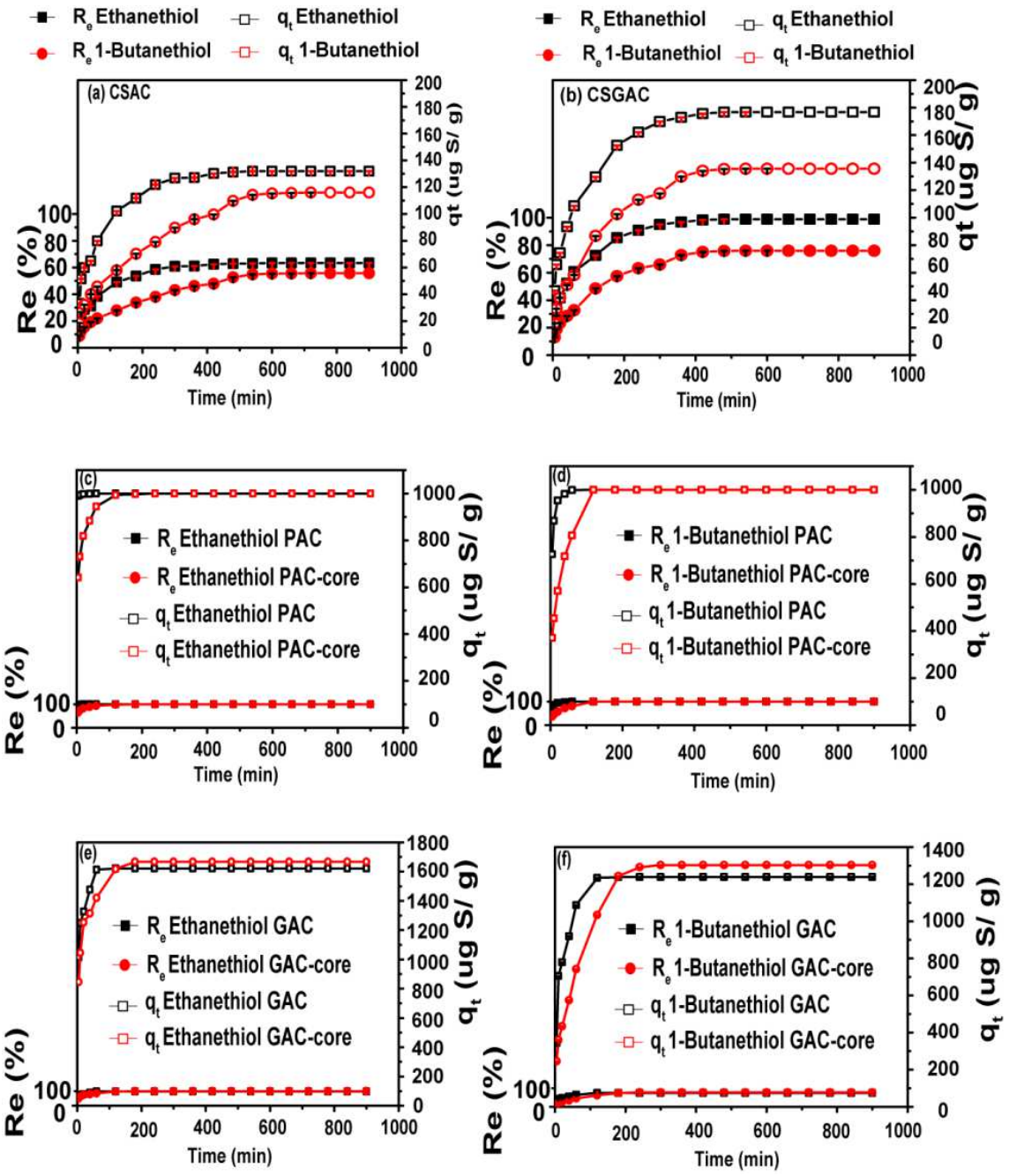
R_e Ethanethiol
q_t Ethanethiol
R_e 1-Butanethiol
q_t 1-Butanethiol
(a) CSAC
(b) CSGAC
Re (%)
qt (ug S/ g)
Time (min)
(c)
R_e Ethanethiol PAC
R_e Ethanethiol PAC-core
q_t Ethanethiol PAC
q_t Ethanethiol PAC-core
(d)
R_e 1-Butanethiol PAC
R_e 1-Butanethiol PAC-core
q_t 1-Butanethiol PAC
q_t 1-Butanethiol PAC-core
(e)
R_e Ethanethiol GAC
R_e Ethanethiol GAC-core
q_t Ethanethiol GAC
q_t Ethanethiol GAC-core
(f)
R_e 1-Butanethiol GAC
R_e 1-Butanethiol GAC-core
q_t 1-Butanethiol GAC
q_t 1-Butanethiol GAC-core

Fig. 4.

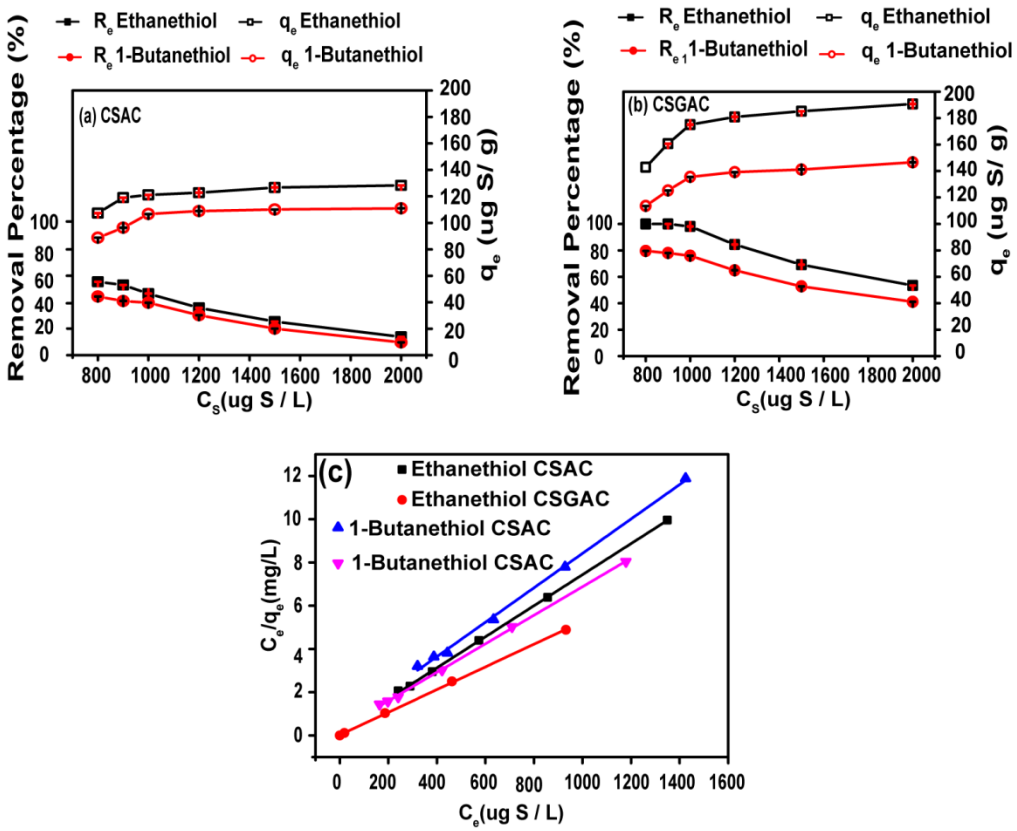

652

653 **Fig. 5.**

654

655

656

657

658

659

660

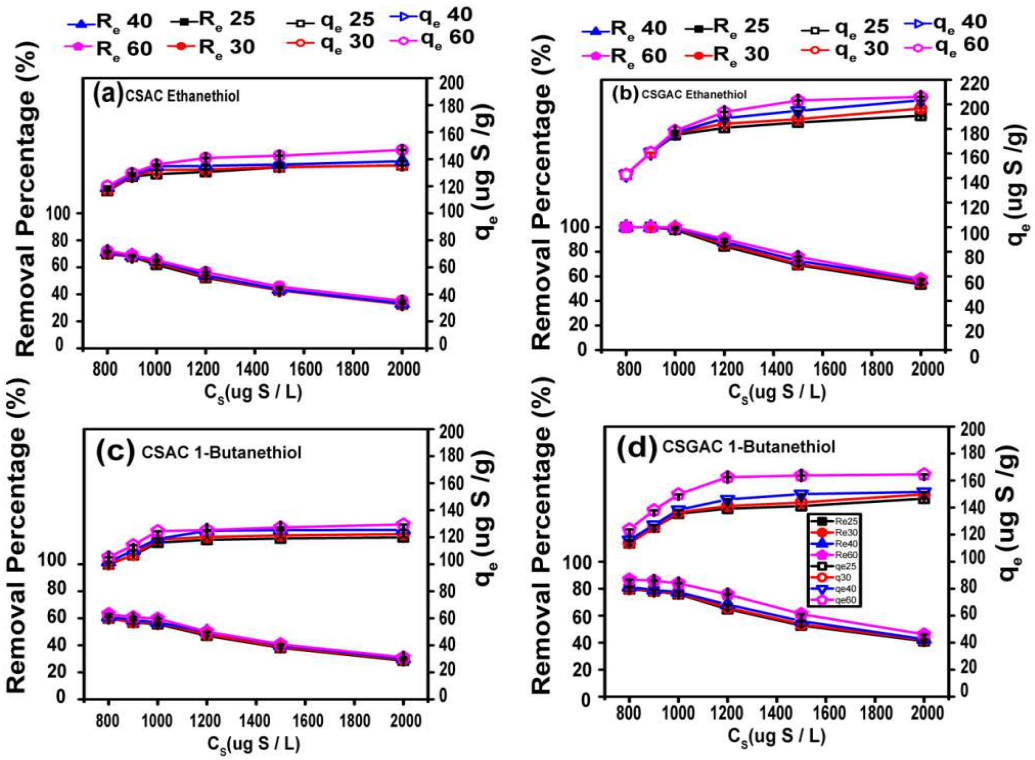
Re 40
Re 25
qe 25
qe 40
Re 60
Re 30
qe 30
qe 60
(a) CSAC Ethanethiol
(b) CSGAC Ethanethiol
(c) CSAC 1-Butanethiol
(d) CSGAC 1-Butanethiol
Removal Percentage (%)
qe (ug S /g)
Cs(ug S / L)
Re25
Re30
Re40
Re60
qe25
qe30
qe40
qe60

Fig. 6.

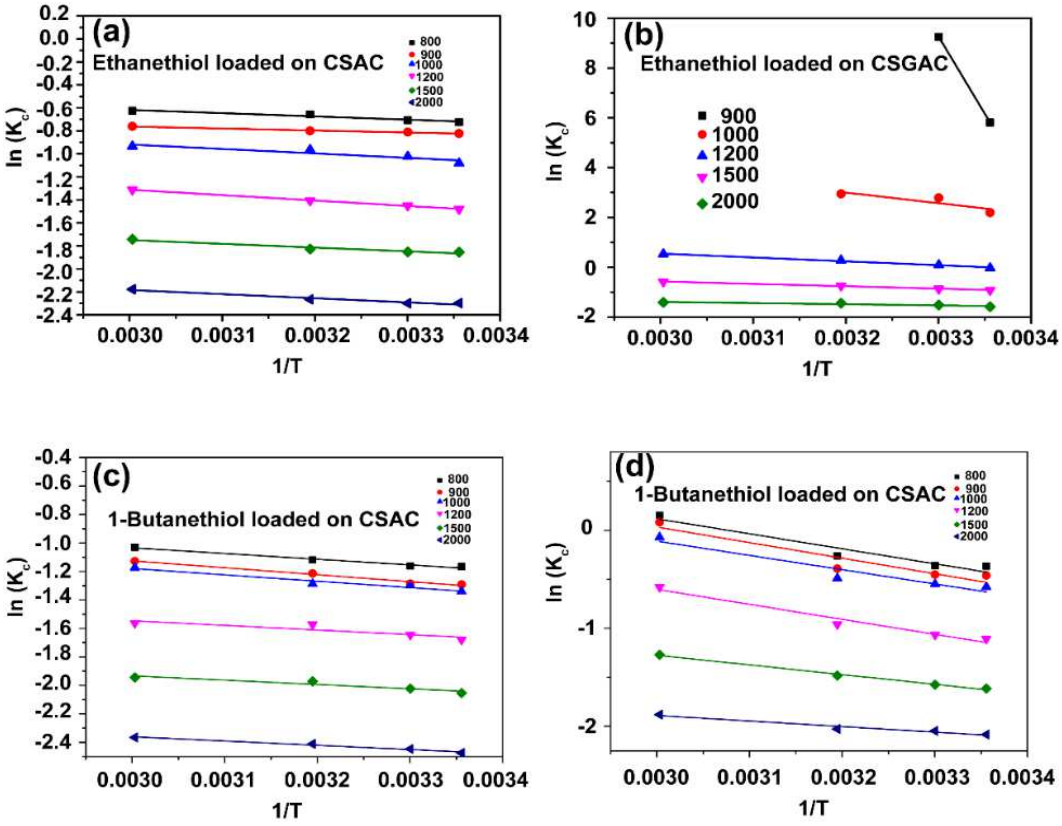

672

673 **Fig. 7.**

674

675

676

677

678

679

680

681

682

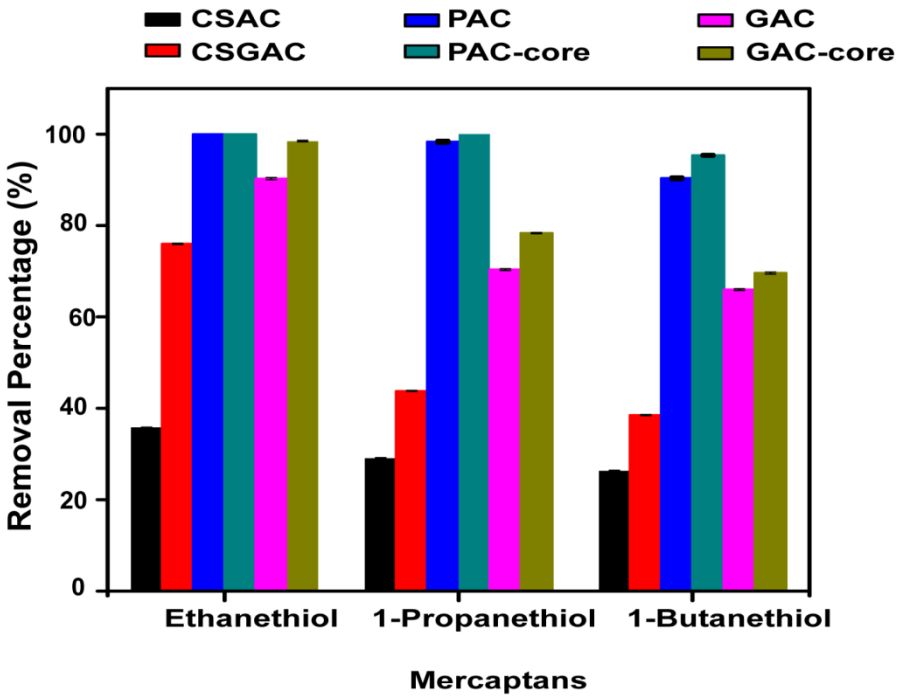

683

684 **Fig. 8**.

685

686

687

688

689

690

691

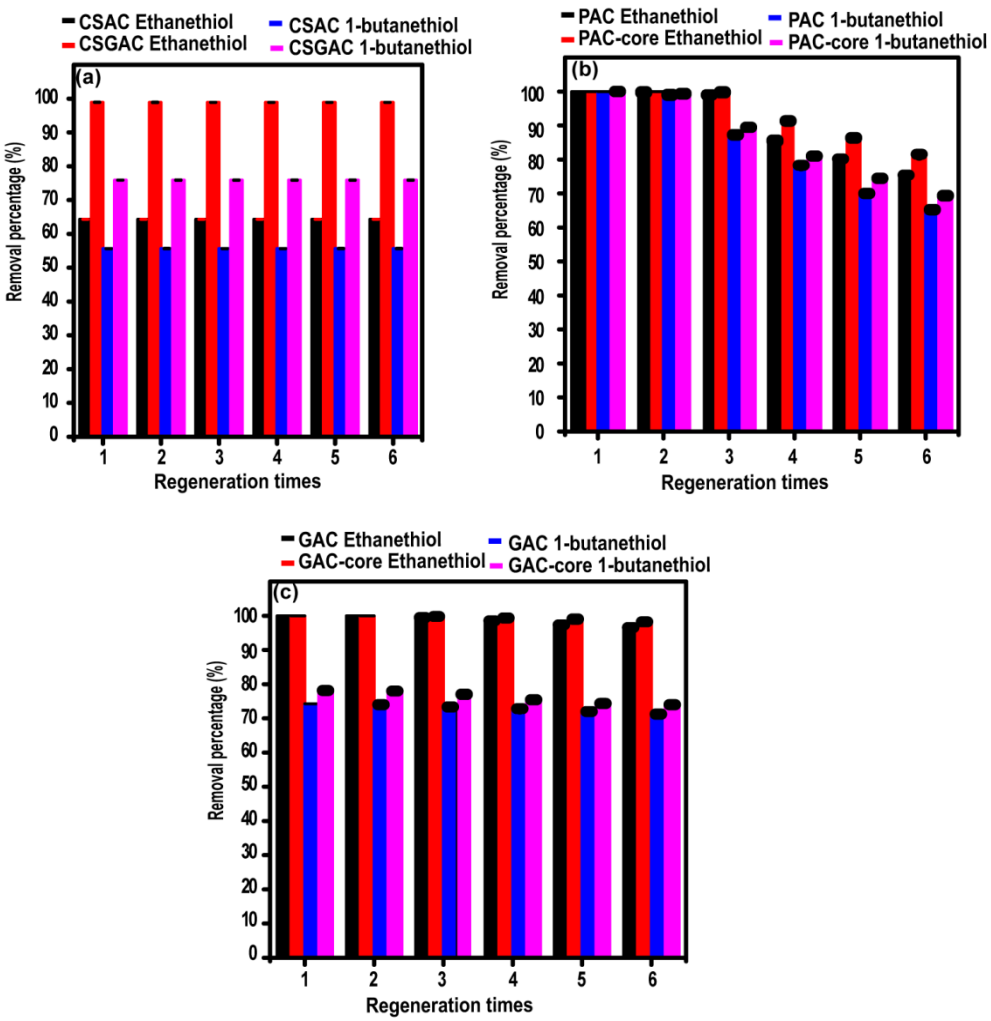

692

693 **Fig. 9.**

694

695

696

697

698

699

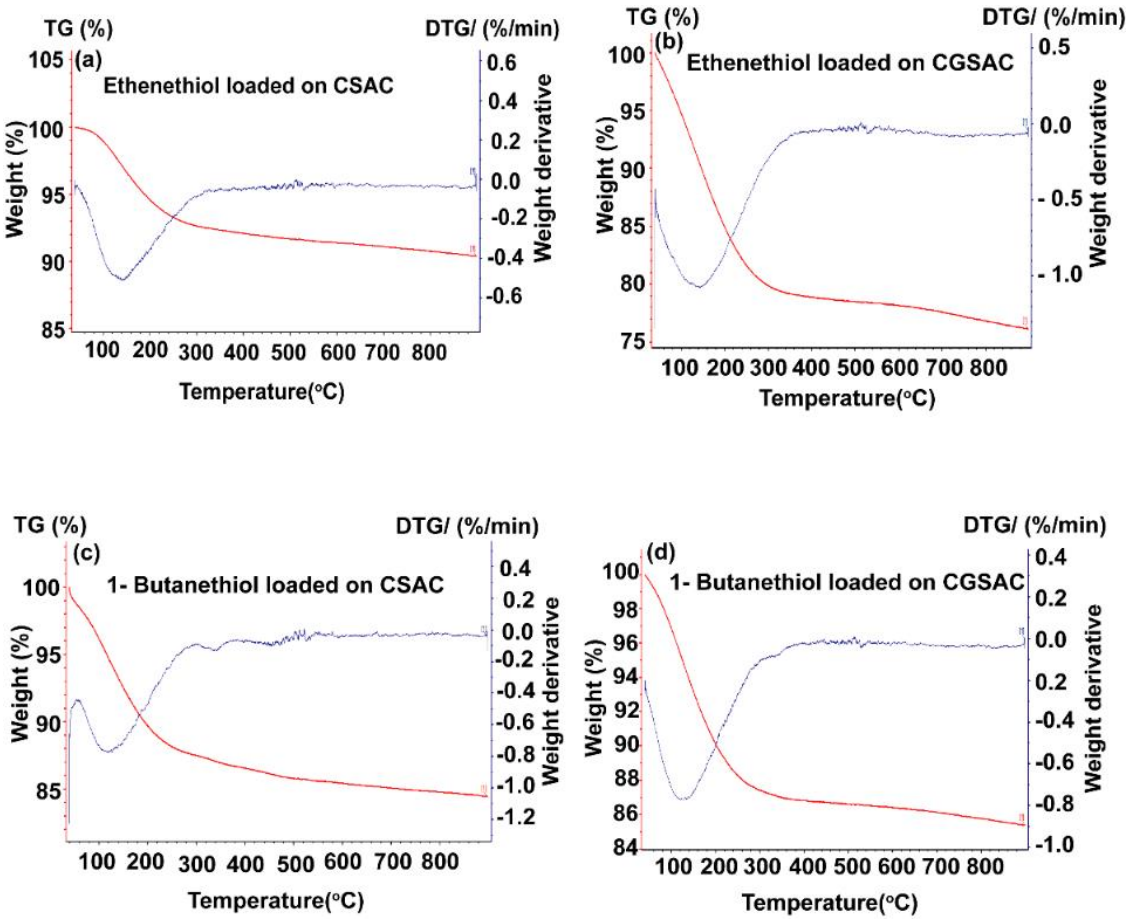
TG (%)
DTG/ (%/min)
(a)
Ethenethiol loaded on CSAC
Weight (%)
Weight derivative
Temperature(°C)
(b)
Ethenethiol loaded on CGSAC
(c)
1- Butanethiol loaded on CSAC
(d)
1- Butanethiol loaded on CGSAC

Fig. 10.

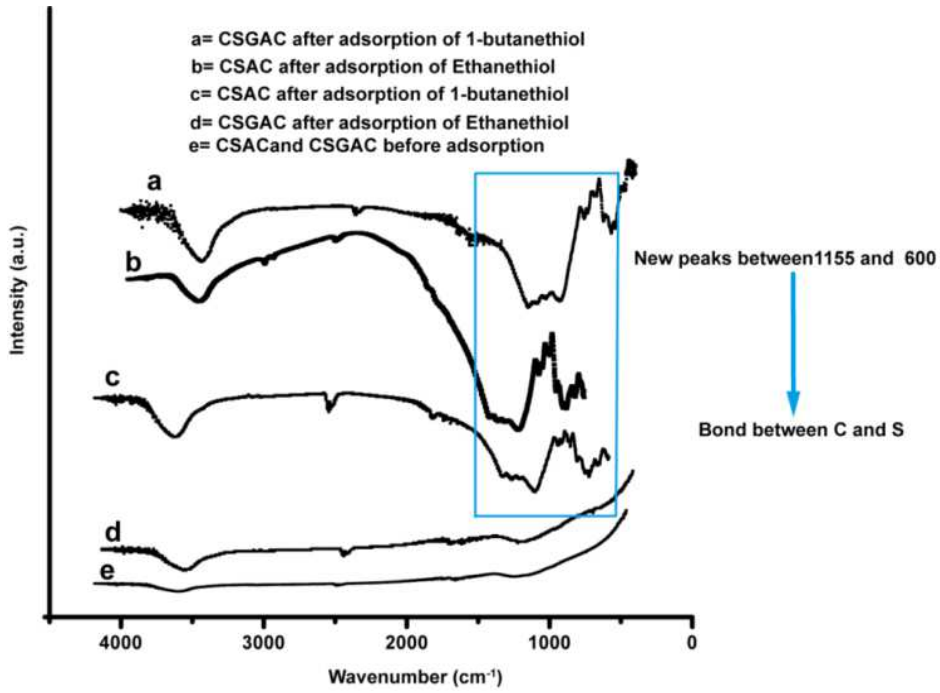
a= CSGAC after adsorption of 1-butanethiol
b= CSAC after adsorption of Ethanethiol
c= CSAC after adsorption of 1-butanethiol
d= CSGAC after adsorption of Ethanethiol
e= CSACand CSGAC before adsorption
a
b
c
d
e
Intensity (a.u.)
4000
3000
2000
1000
0
Wavenumber (cm-1)
New peaks between1155 and 600
Bond between C and S

Fig. 11.

Figures

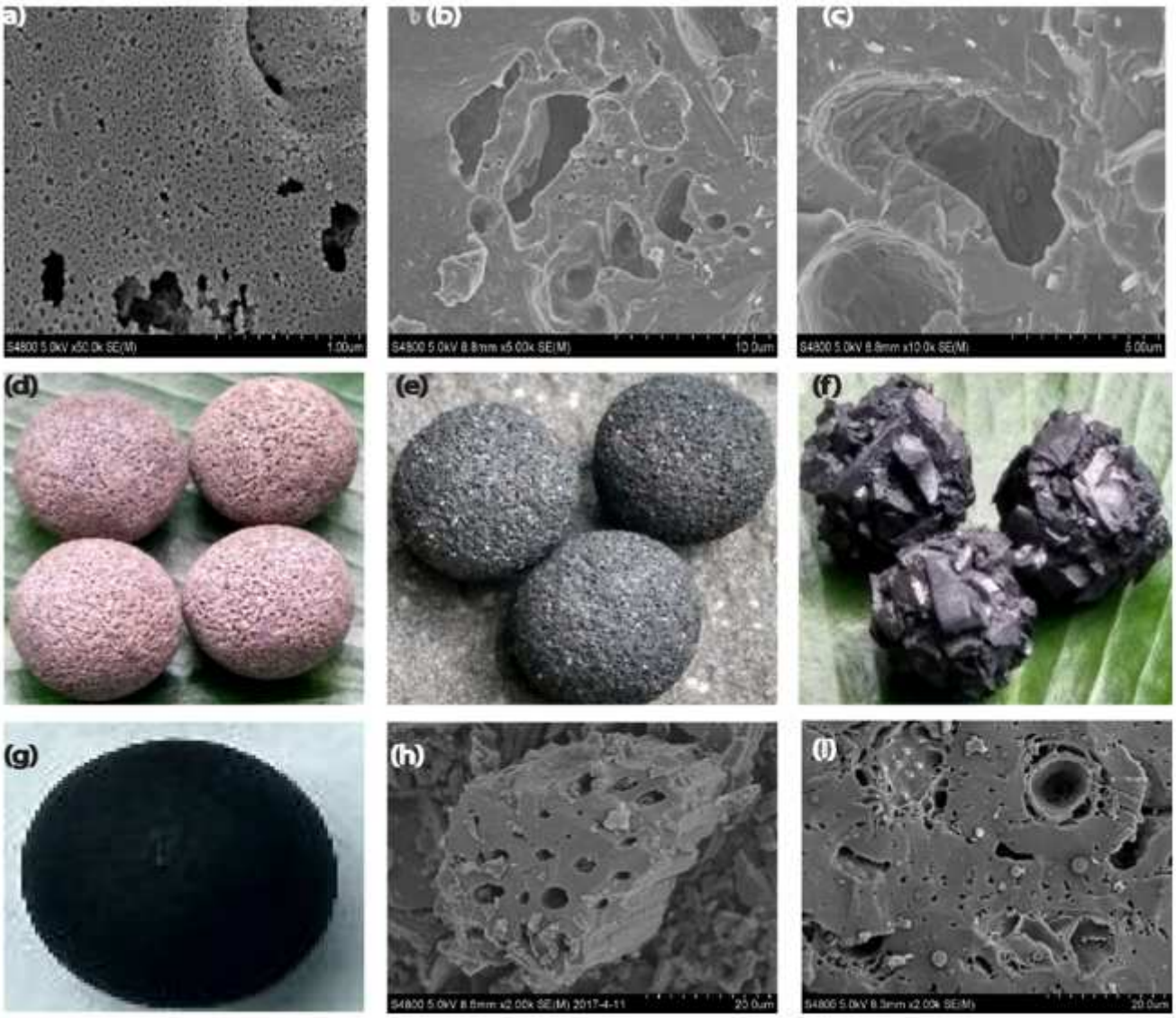

Figure 1

SEM images of shell (a), intra-particle space or void in shell of CSAC (b), CSGAC (c), physical images of CSAC (d), CSGAC (e), GAC-core (f), PAC-core (g), SEM images of PAC-core (h), and GAC-core (i).

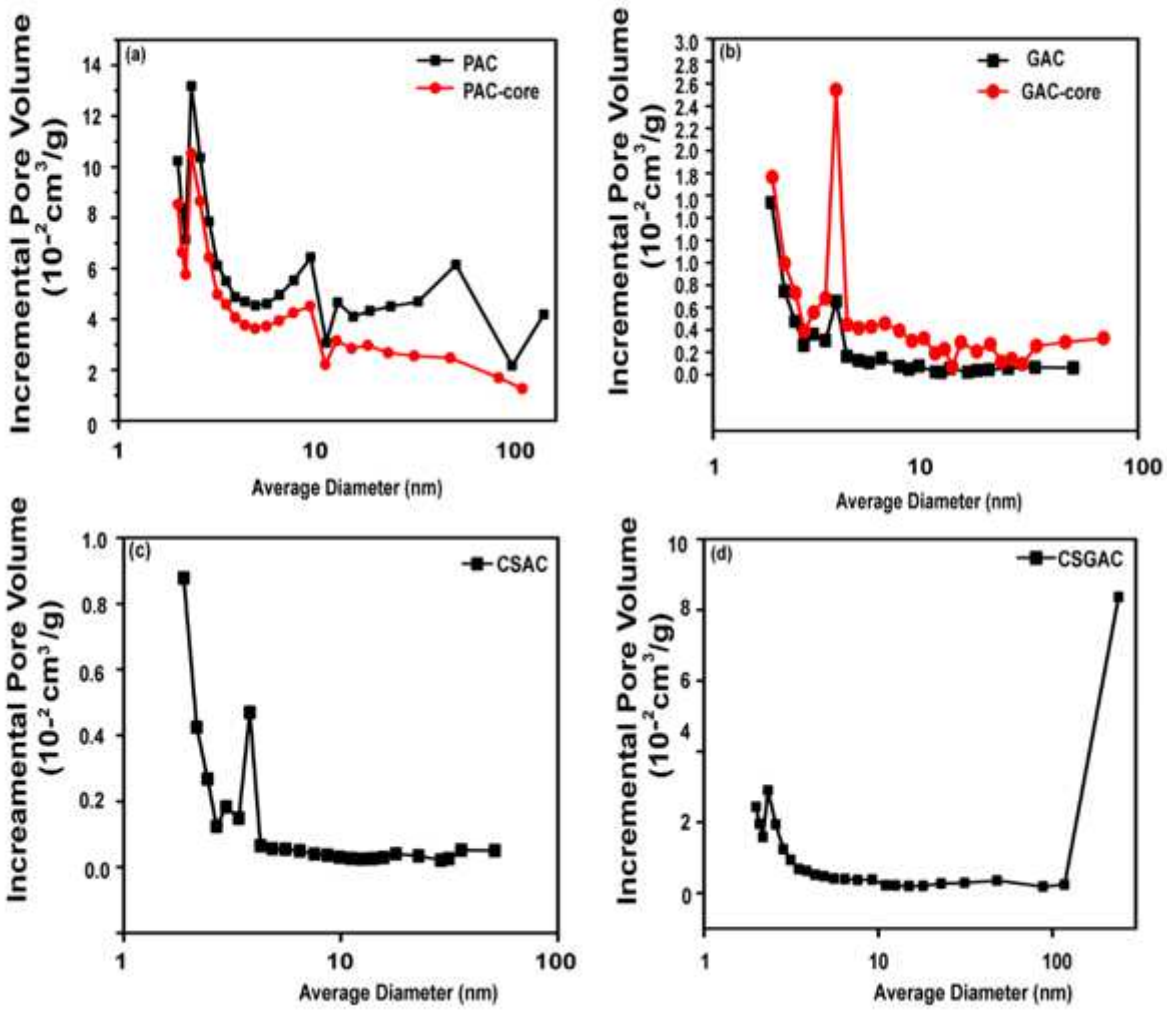

Figure 2

The pore distribution of PAC-based adsorbent (a), GAC-based adsorbent (b), and core-shell ACs (c, d).

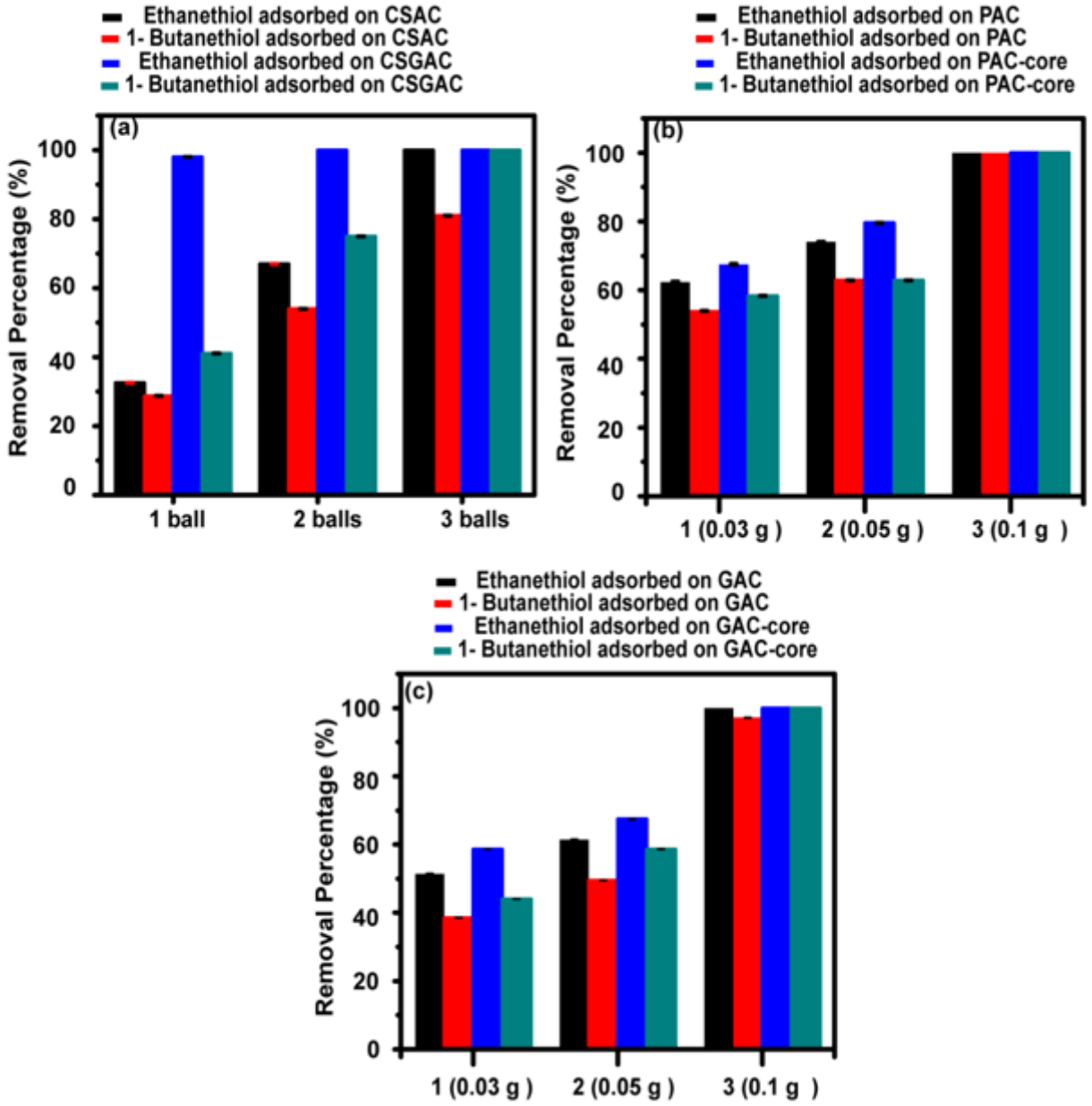

Figure 3

Effect of adsorbent dosage on the mercaptans removal by CSAC and CSGAC (a), PAC-based adsorbents (b), and GAC-based adsorbents(c). (Conditions: C0 = 2000 ppm, V = 50 mL, mass = 0.24 g (CSAC), 0.28 g (CSGAC), 0.05 g (PAC-core and PAC), and 0.03 g (GAC-core and GAC)).

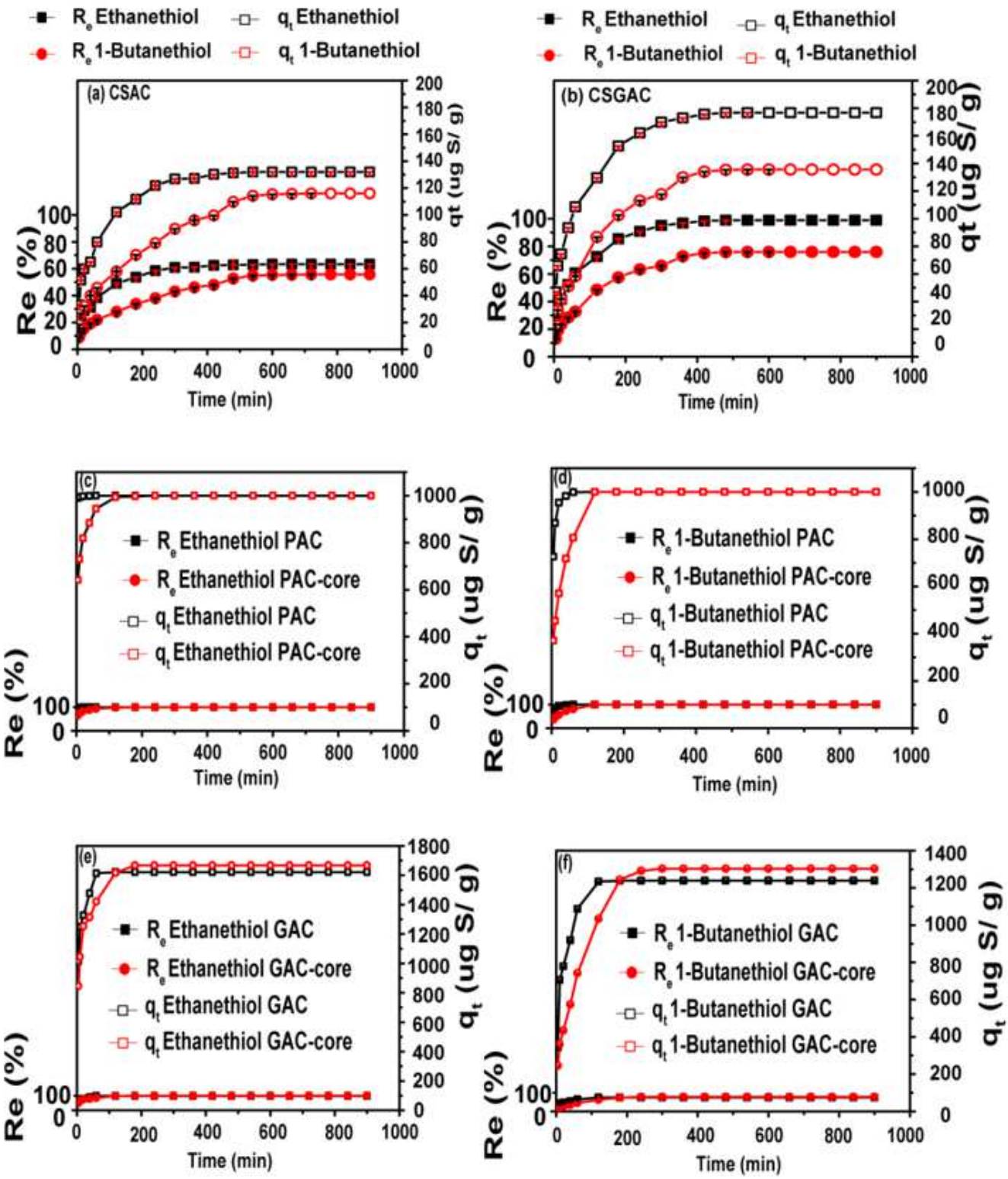

Figure 4

Effect of contact time for CSAC and CSGAC (a, b) and for PAC, PAC-core, GAC, GAC–core (c-f). (Conditions: C0 = 1000 ppm, V = 50 mL, mass = 0.24 g (CSAC), 0.28 g (CSGAC), 0.05 g (PAC-core and PAC) and 0.03 g (GAC-core and GAC).

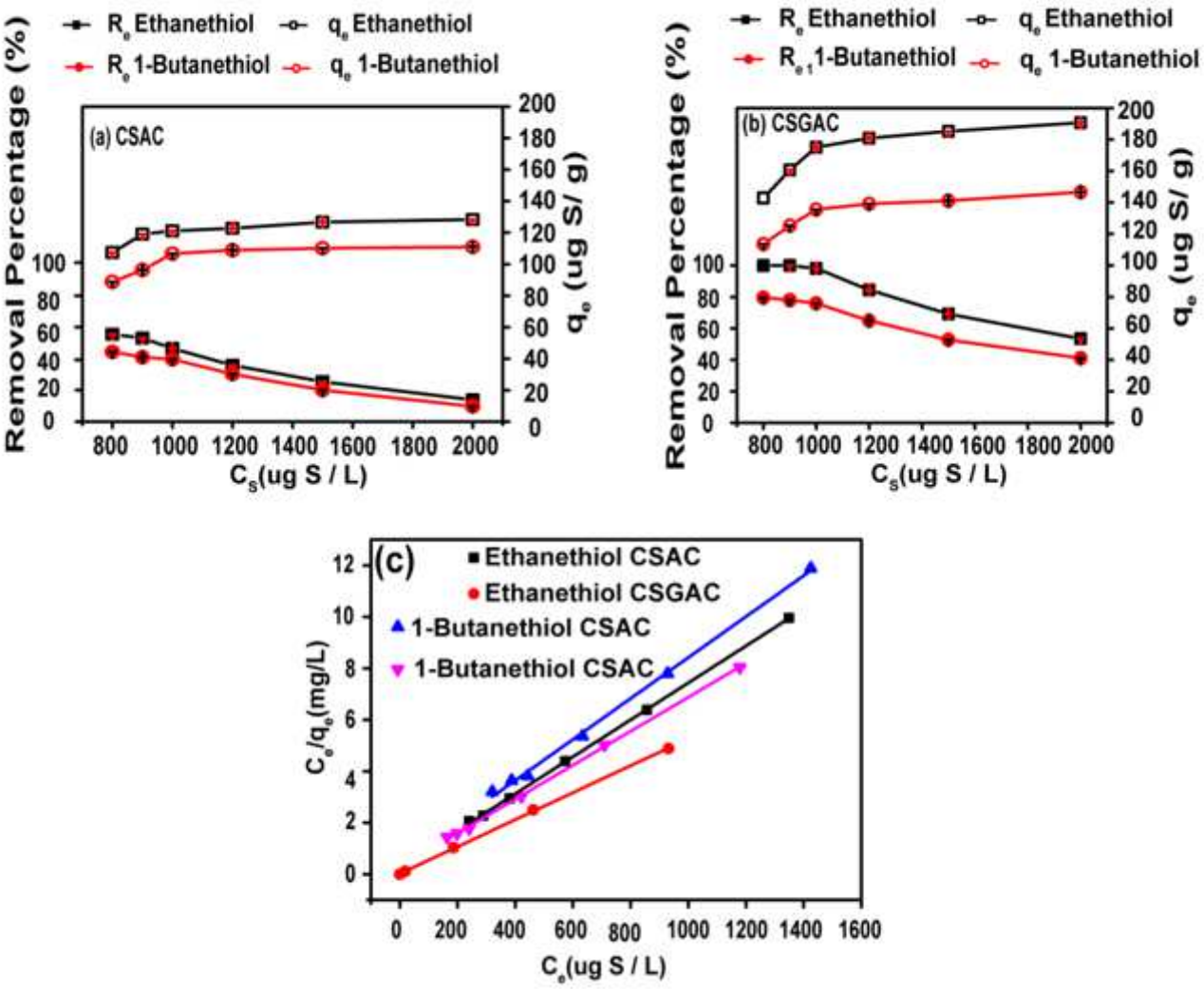

Figure 5

Effect of initial concentration on mercaptans removal (a, b), and Langmuir fitting model (c)

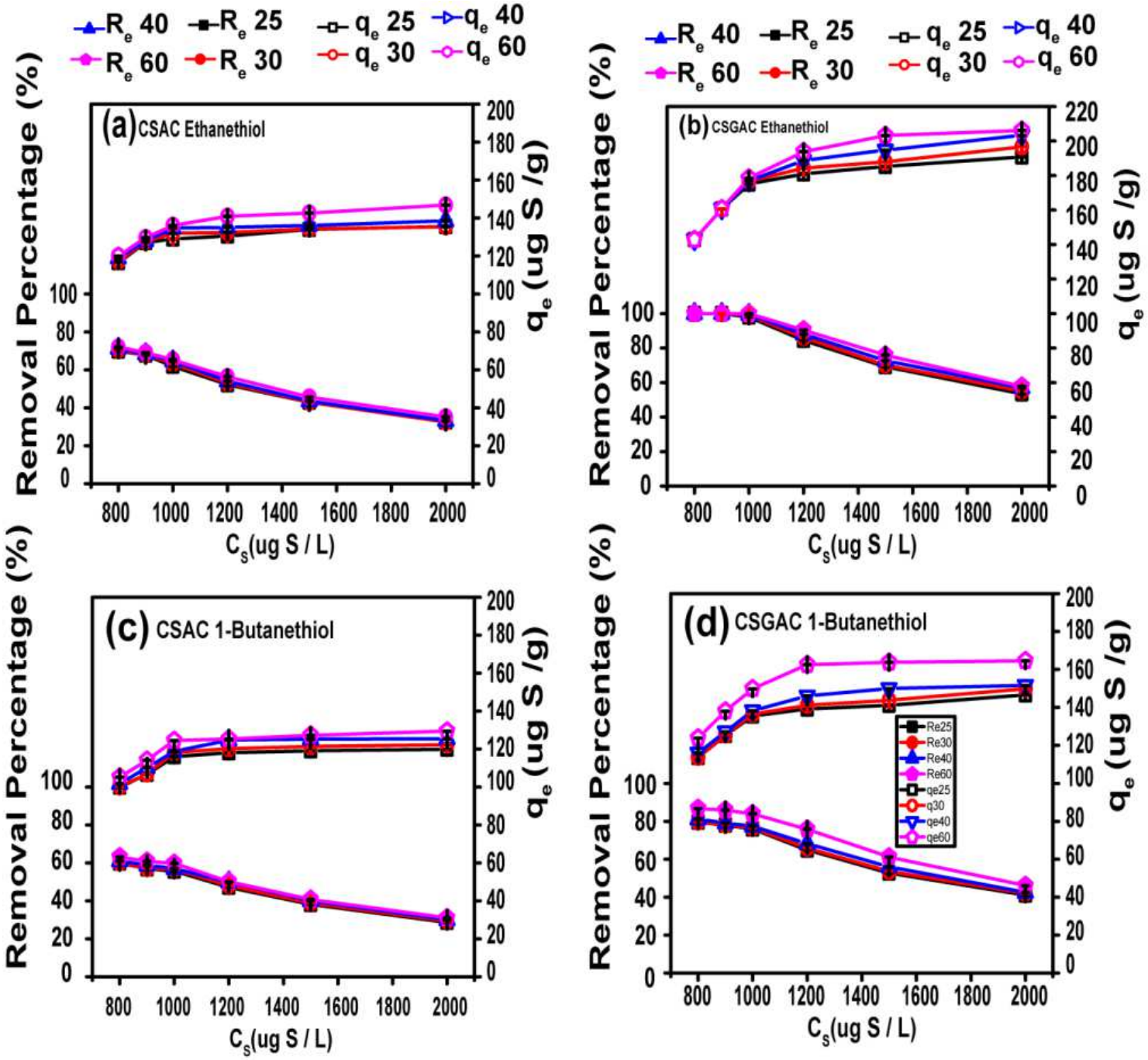

Figure 6

Temperature effect: Ethanethiol adsorbed on CSAC and CSGAC (a, b), 1-Butanethiol adsorbed on CSAC and CSGAC (c, d).

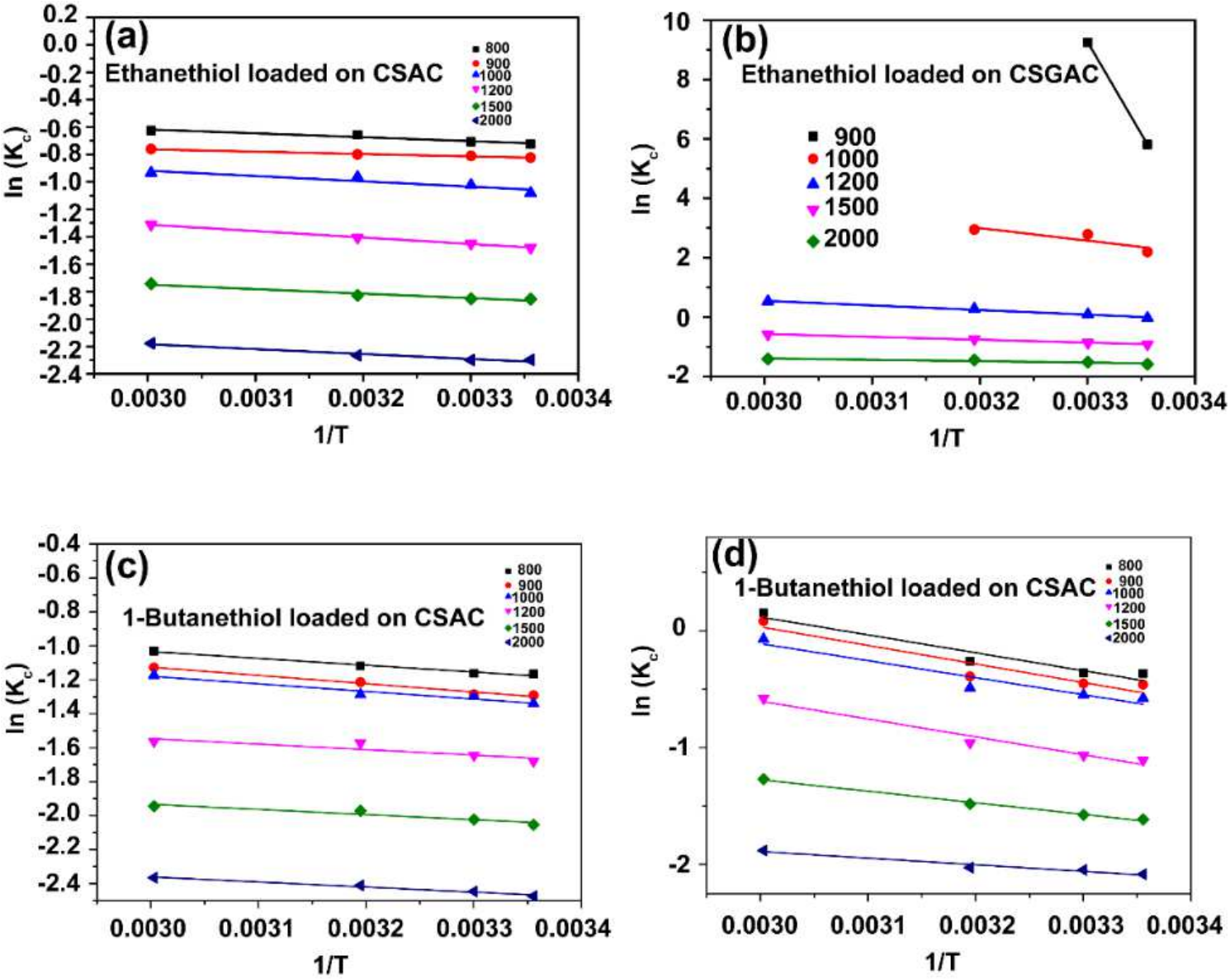

Figure 7

The plot of KC versus 1/T for determination of mercaptans removal reaction enthalpy.

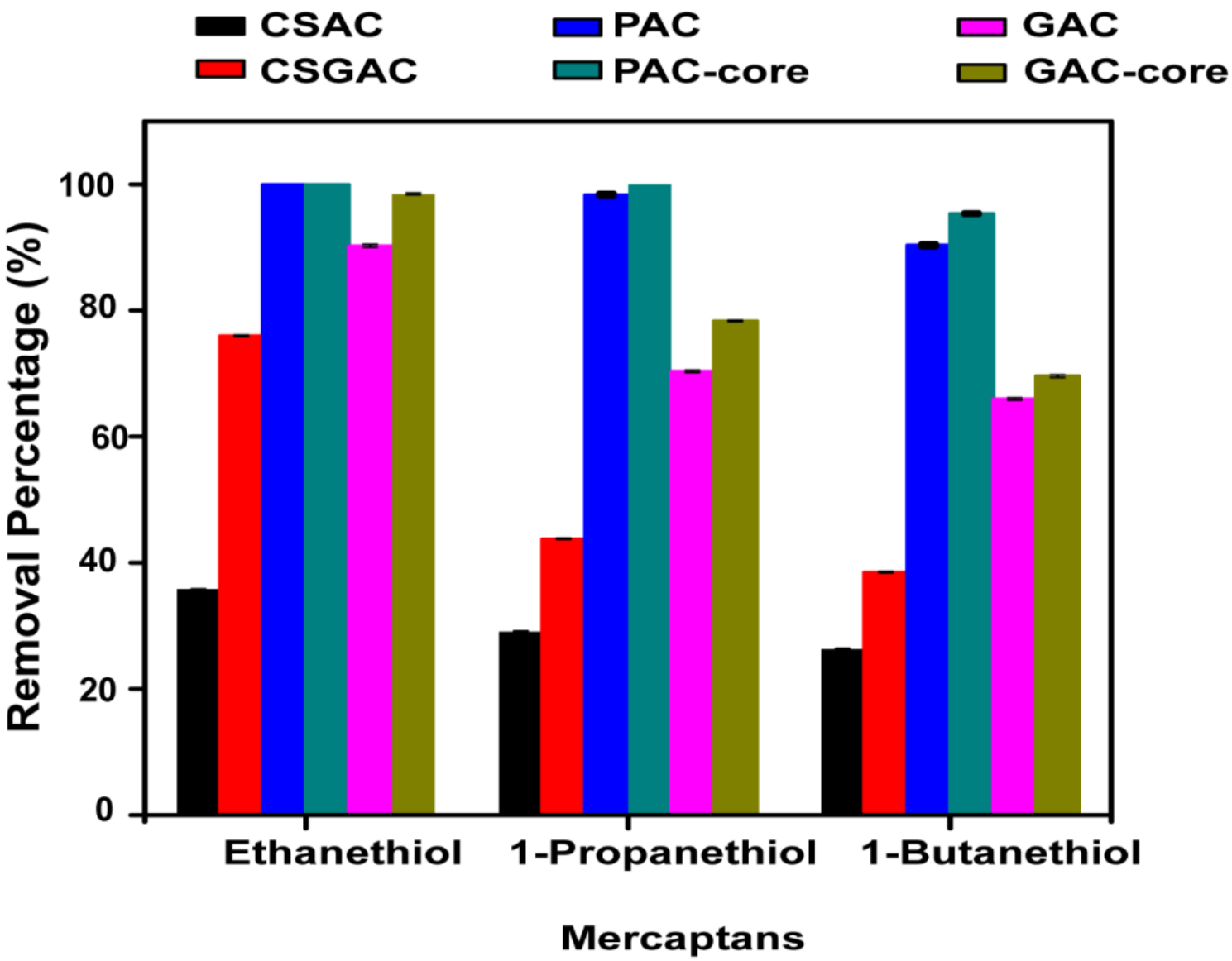

Figure 8

Adsorption competition of mercaptans by core- shell ACs, PAC-based adsorbents and GAC-based adsorbents. (Conditions: C0= 1000 ppm, V= 50 mL, mass= 0.24 g (CSAC), 0.28 g (CSGAC), 0.05 g (PAC-core and PAC) and 0.03 g (GAC-core and GAC).

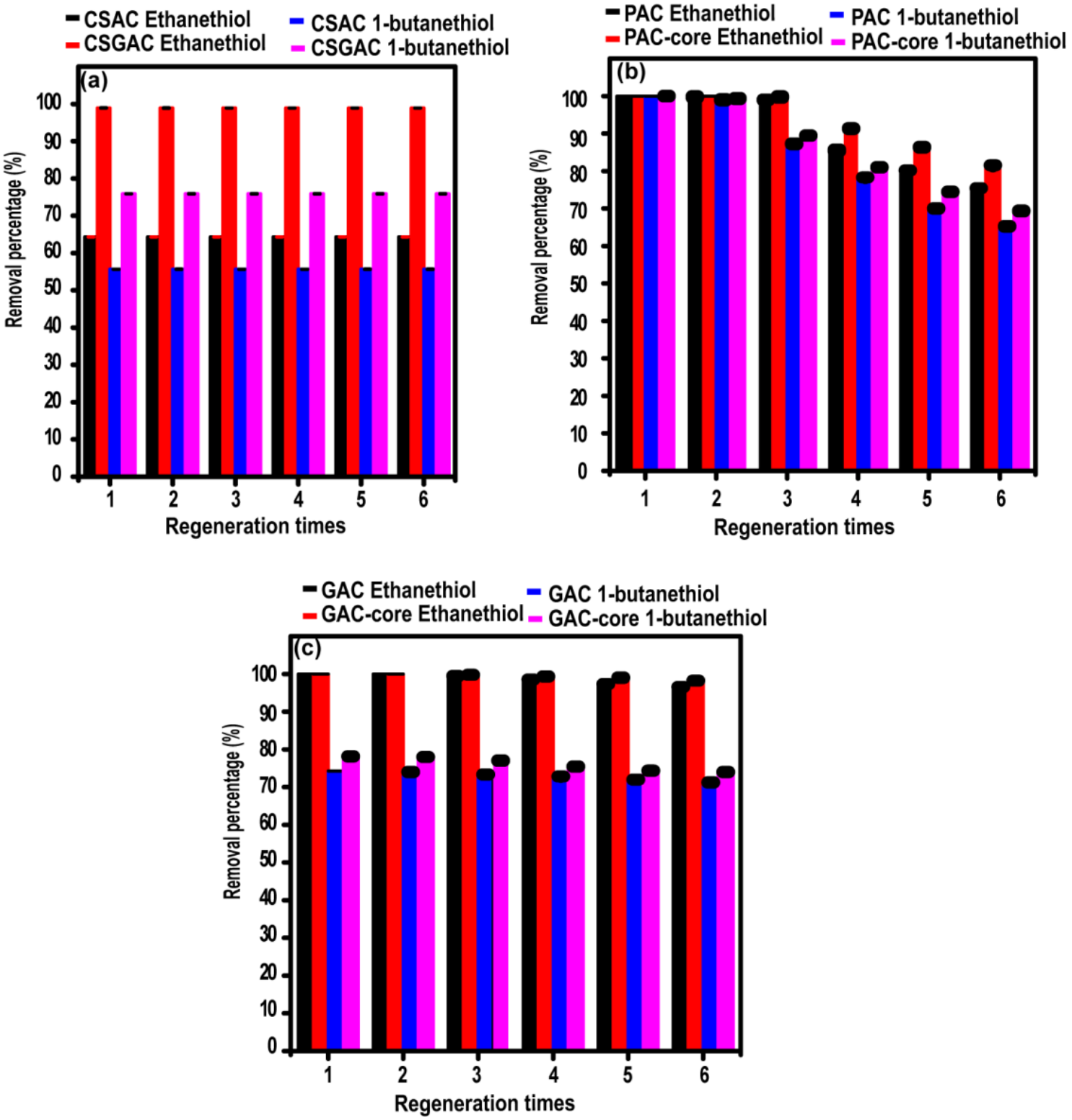

Figure 9

Thermal regeneration of mercaptans by core-shell AC (a) and PAC and GAC based adsorbents (b, c).

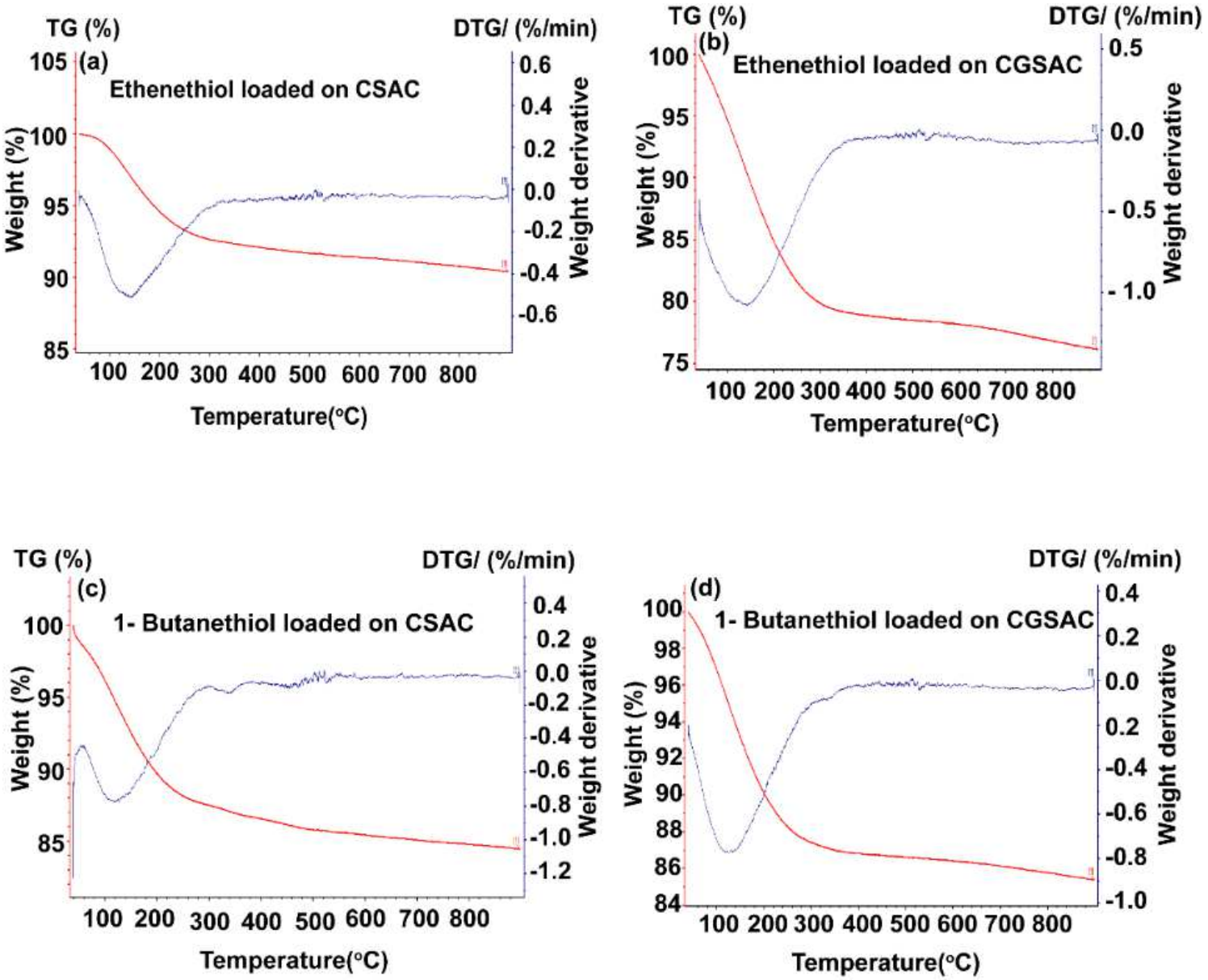

Figure 10

TG and DTG curves of treated CSAC and CSGAC.

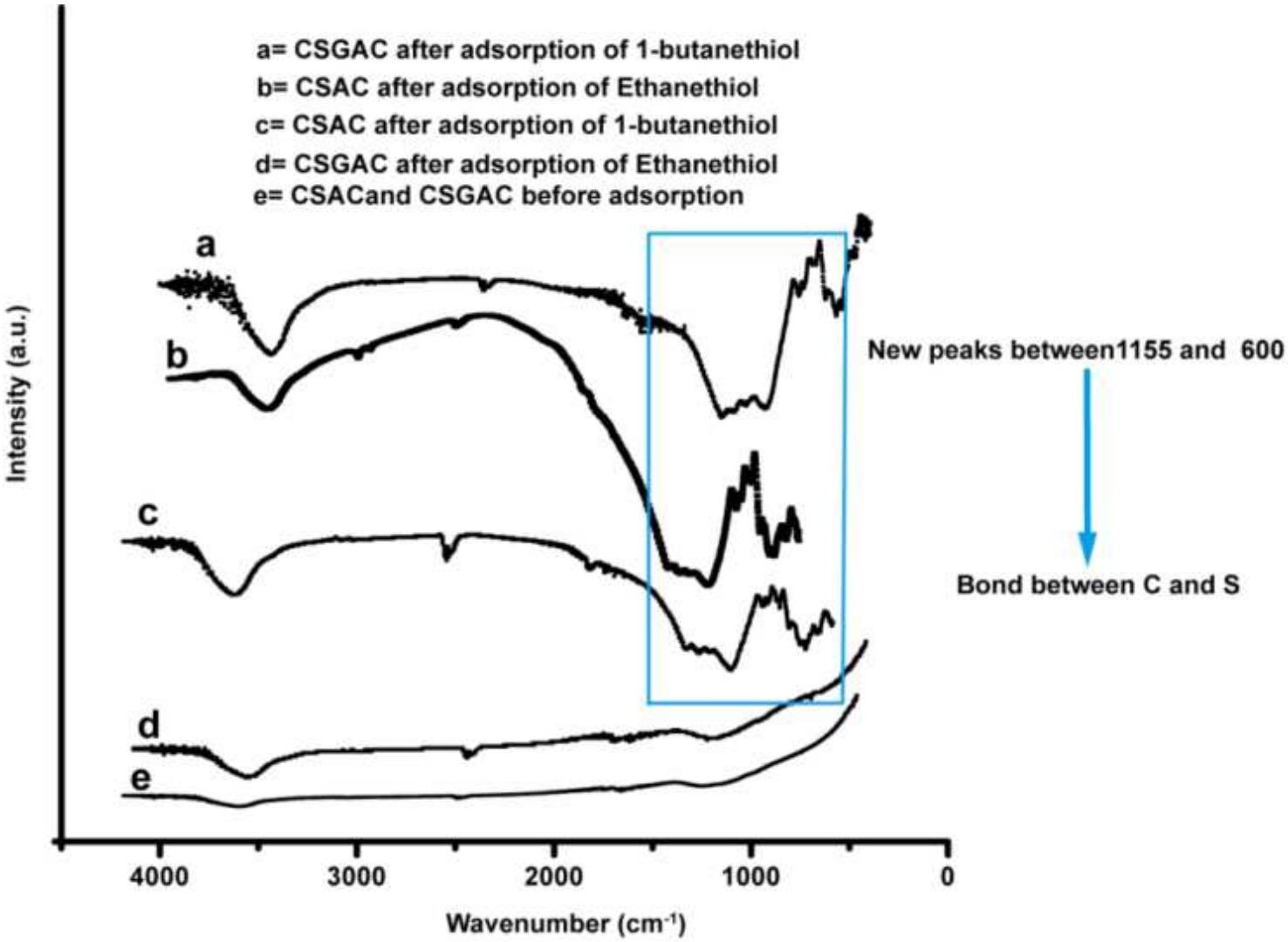

Figure 11

FTIR spectra of pristine and treated CSAC and CSGAC.

Supplementary Files

This is a list of supplementary files associated with this preprint. Click to download.

- GraphicalAbstract.png
- Supplementarymaterial.docm